

UNCLASSIFIED

AD NUMBER
AD923913
NEW LIMITATION CHANGE
TO Approved for public release, distribution unlimited
FROM Distribution authorized to U.S. Gov't. agencies only; Test and Evaluation; Sep 1974. Other requests shall be referred to Director, Ballistic Research Lab., Aberdeen Proving Ground, MD 21005.
AUTHORITY
USAARDC ltr, 8 Mar 1978

THIS PAGE IS UNCLASSIFIED

AD 923913L

BRL MR 2411

BRL

MEMORANDUM REPORT NO. 2411

YAWING AND BALLOTING MOTION OF A
PROJECTILE IN THE BORE OF A GUN WITH
APPLICATION TO GUN TUBE DAMAGE

Evan Harris Walker

PROPERTY OF U.S. ARMY
STINNING BRANCH
BRL, ABERDEEN, MD. 21005

September 1974

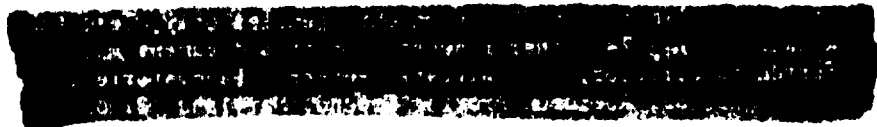
Approved for public release; distribution unlimited.

USA BALLISTIC RESEARCH LABORATORIES
ABERDEEN PROVING GROUND, MARYLAND

Destroy this report when it is no longer needed.
Do not return it to the originator.

Secondary distribution of this report by originating
or sponsoring activity is prohibited.

Additional copies of this report may be obtained
from the Defense Documentation Center, Cameron
Station, Alexandria, Virginia 22314.



The findings in this report are not to be construed as
an official Department of the Army position, unless
so designated by other authorized documents.

SECURITY CLASSIFICATION OF THIS PAGE (When Data Entered)

REPORT DOCUMENTATION PAGE		READ INSTRUCTIONS BEFORE COMPLETING FORM
1. REPORT NUMBER BRL Memorandum Report No. 2411	2. GOVT ACCESSION NO.	3. RECIPIENT'S CATALOG NUMBER
4. TITLE (and Subtitle) YAWING AND BALLOTING MOTION OF A PROJECTILE IN THE BORE OF A GUN WITH APPLICATION TO GUN TUBE DAMAGE		5. TYPE OF REPORT & PERIOD COVERED Final
		6. PERFORMING ORG. REPORT NUMBER
7. AUTHOR(s) Evan Harris Walker		8. CONTRACT OR GRANT NUMBER(s)
9. PERFORMING ORGANIZATION NAME AND ADDRESS USA Ballistic Research Laboratories Aberdeen Proving Ground, Maryland 21005		10. PROGRAM ELEMENT, PROJECT, TASK AREA & WORK UNIT NUMBERS
11. CONTROLLING OFFICE NAME AND ADDRESS U.S. Army Materiel Command 5001 Eisenhower Avenue Alexandria, Virginia 22333		12. REPORT DATE SEPTEMBER 1974
		13. NUMBER OF PAGES 59
14. MONITORING AGENCY NAME & ADDRESS (if different from Controlling Office)		15. SECURITY CLASS. (of this report) UNCLASSIFIED
		15a. DECLASSIFICATION/DOWNGRADING SCHEDULE
16. DISTRIBUTION STATEMENT (of this Report) <div style="text-align: center; border: 1px solid black; padding: 5px;">Approved for public release; distribution unlimited.</div>		
17. DISTRIBUTION STATEMENT (of the abstract entered in Block 20, if different from Report)		
18. SUPPLEMENTARY NOTES		PROPERTY OF U.S. ARMY SHIPPING BRANCH BRL, AFG, MD. 21005
19. KEY WORDS (Continue on reverse side if necessary and identify by block number) Interior Ballistics Launching Balloting Model, yawing-in-bore Side-Slap Premature Bore-riding Muzzle wear		
20. ABSTRACT (Continue on reverse side if necessary and identify by block number) (mba) New basic Equations of motion are derived to describe in bore shell yawing and balloting motion. It is shown that the prior equations of Reno and Thomas are not satisfactory. These equations are used to derive expressions for the growth of balloting motion. Application of these equations to a mechanical failure of a shell in an 8" howitzer XM201 test program shows the new treatment accounts for the observed tube damage. This approach provides a basis for calculating causes and probability of occurrences of severe balloting.		

UNCLASSIFIED

SECURITY CLASSIFICATION OF THIS PAGE(When Data Entered)



UNCLASSIFIED

SECURITY CLASSIFICATION OF THIS PAGE(When Data Entered)

SUMMARY

New equations for the yawing and balloting motion of a projectile in the bore of a gun have been derived. These equations show that the previous theories of Reno and Thomas omitted important forces acting to cause in some cases severe buildup of balloting motion. These equations also show the prior treatment to be unsatisfactory even where severe balloting does not occur. The new equations will be used to compute the details of shell in bore motion in a subsequent report.

In the present report, the general equations for shell in bore motion have been used to derive equations describing specifically the growth of balloting motion to show how balloting can build to severe levels causing tube damage. These equations also make possible a calculation of the occurrence probability for severe balloting and allow one to determine important factors contributing to mechanical failures and prematures.

Balloting motion is also important in causing severe shell engraving and wearing of gun tubes. Thus control of balloting motion should significantly increase the service life of gun tubes.

The theoretical equations have been applied to the calculation of balloting in the XM201 8" Howitzer tube. Agreement between observed damage and the results of computations is obtained in these calculations.

TABLE OF CONTENTS

	Page
ABSTRACT	1
SUMMARY	3
LIST OF ILLUSTRATIONS	7
I. INTRODUCTION	9
II. THE EQUATIONS OF MOTION	10
III. GROWTH OF ENERGY IN THE TRANSVERSE MODE	18
IV. INITIAL MOTION OF THE PROJECTILE	25
V. CALCULATION OF THE COEFFICIENT OF RESTITUTION	27
VI. APPLICATION TO THE 8" HOWITZER TUBE XM201 MECHANICAL FAILURE OF APRIL 11, 1974	32
REFERENCES	38
APPENDIX I - EQUIPMENT PERFORMANCE REPORT FOR 8" HOWITZER TUBE XM201 MECHANICAL FAILURE OF APRIL 15, 1974	39
LIST OF SYMBOLS	51
DISTRIBUTION LIST	57

LIST OF ILLUSTRATIONS

Figure	Page
1. Euler's angles, δ , ϕ , λ , specifying the orientation of a symmetrical shell about a point C at the center of the rotating band on the shell axis	11
2. Sketch of the region of contact between the gun tube bore and the rotating band of a shell	14
3. Calculation of balloting energy ϵ as a function of shell position s in the 8" Howitzer tube for a zone 9 charge as computed using Eq. (80) and the results of the integration of Eq. (85).	26
4. Plot of the energy ϵ_0 in the balloting mode at first impact with the gun bore as a function initial shell altitude (yaw angle δ_0 divided by the maximum yaw angle Δ) as computed from Eq. (85) for the 8" M106 HE shell launched with a zone 9 charge in the XM201 Howitzer tube	28
5. Plot of the pressure time curves computed by L.D. Heppner of MTD for the 8" M106 HE shell launched with an XM188 zone 9 charge at -70°F in the XM201 Howitzer tube.	29
6. Plot of the energy ϵ in the balloting mode at the muzzle of the gun tube as a function of the initial shell altitude (initial yaw angle divided by the maximum possible yaw) computed from Eqs (80) and (101) using the results the integration of Eq (85) shown in Figure 4 and with a coefficient of restitution e of 0.7 and $\gamma = 140.6$ as appropriate for the conditions of the 8" M106 HE shell at -70°F , the XM188 zone 9 charge at -70°F fired in the XM201 Howitzer tube.	36
A-1. Photograph of damage to the 8" XM201 Howitzer tube looking from the muzzle end	45
A-2. Plot of the pressure difference between strain gage #1 at the spindle and strain gage #3 at the forcing cone as a function of time	49
A-3. Plot of the pressure vs. time for three tourmaline strain gages located at the spindle (#1, 10" RFT), middle of chamber (#2, 29.65" RFT) and at the forcing cone (#3, 42.90" RFT)	50

I. INTRODUCTION

This report stems from an investigation of a shell failure that occurred while testing the 8-inch howitzer tube XM201. The characteristics of the damage to the tube indicated that the shell, before breaking up, balloted with sufficient violence to cause impact shearing of lands in three separate sections of the tube. This tube damage will be considered in more detail below.

A consideration of the Reno^{1*} and Thomas² theories of shell motion in a gun tube and Gay's³ application of those theories indicates that they do not predict conditions that would lead to violent motion of the shell. Gay found that these theories predict that the yawing motion of the shell will bring the shell bourrelet into contact with the lands (if not initially resting against the tube wall) early in the motion of the shell and that yawing motion will be rapidly damped. The speed of the bourrelet approaching the lands is never large. For a coefficient of restitution $e = 1$, a bourrelet clearance of 0.02 inch (a large clearance) and using Reno's equations (which give slightly larger values than Thomas'), Gay's calculations give (see his Figure 4) 60.0 cm/sec (1.97 ft/sec). This is not a significant speed; the 8-inch shell which broke up in the tube had passed a 7-foot drop test (velocity at impact, 647 cm/sec) and impact against the lands of the gun tube at such speeds will not cause damage.

Other evidence cited by Gay would also suggest that severe balloting has been a recurring problem. Gay shows (his Figure 12) a 105mm shell in flight beside the broken-off fuze. The engraving noted on 8-inch shell at the bourrelet also indicates that balloting frequently exceeds that predicted by the theoretical treatments.

One should expect, however, that under appropriate conditions an instability in the motion of a shell driven by a force acting behind the shell's center of gravity (c.g.) should occur. Such a motion should resemble "chatter" that occurs in other mechanical systems. The following analysis shows that the treatment given by Thomas requires modification to incorporate the forces acting on the shell at the rotating band and a minor correction to the form of the equations giving constants of the motion. The treatment given here is also somewhat more general in that it incorporates certain significant effects on the shell motion due to the elastic nature of the shell.

By taking the time average contribution of the impact to the lateral motion of a shell, it is possible to derive closed form expressions for the growth of balloting and show what parameters of this motion favor its occurrence.

*References are listed on page 38.

II. THE EQUATIONS OF MOTION

We follow the procedure after Goldstein⁴ for the similar problem of the motion of a symmetric top supported at one point and acted on by gravity. The Lagrangian procedure is used to obtain the equations of motion. Since the shell may be taken to be symmetric about its axis (also assumed by Reno and by Thomas), the kinetic energy can be written as

$$T = \frac{1}{2} I(\omega_y^2 + \omega_z^2) + \frac{1}{2} A\omega_x^2, \quad (1)$$

where ω_x , ω_y , ω_z are the angular velocities about the respective axis and I is given by

$$I = B + m\ell^2, \quad (2)$$

where A and B are the axial and transverse moments of inertia of the shell about the c.g., m is the mass of the shell, and ℓ is the distance from the point C to the c.g. as indicated in Figure 1. In terms of the Euler angles, this is

$$T = \frac{1}{2} I(\dot{\delta}^2 + \dot{\phi}^2 \sin^2 \delta) + \frac{1}{2} A(\dot{\psi} + \dot{\phi} \cos \delta)^2. \quad (3)$$

In a coordinate system moving with the point C and subject to the acceleration \ddot{s} of the projectile, there exists an instantaneous potential field for the projectile given by

$$V = m\ddot{s} \ell \cos \delta. \quad (4)$$

The Lagrangian is

$$L = T - V, \quad (5)$$

and the Lagrangian equation is

$$\frac{d}{dt} \frac{\partial L}{\partial \dot{q}_i} - \frac{\partial L}{\partial q_i} = Q_i; \quad i = 1, 2, 3 \quad (6)$$

where

$$\begin{aligned} q_1 &= \delta \\ q_2 &= \phi \\ q_3 &= \psi \end{aligned} \quad (7)$$

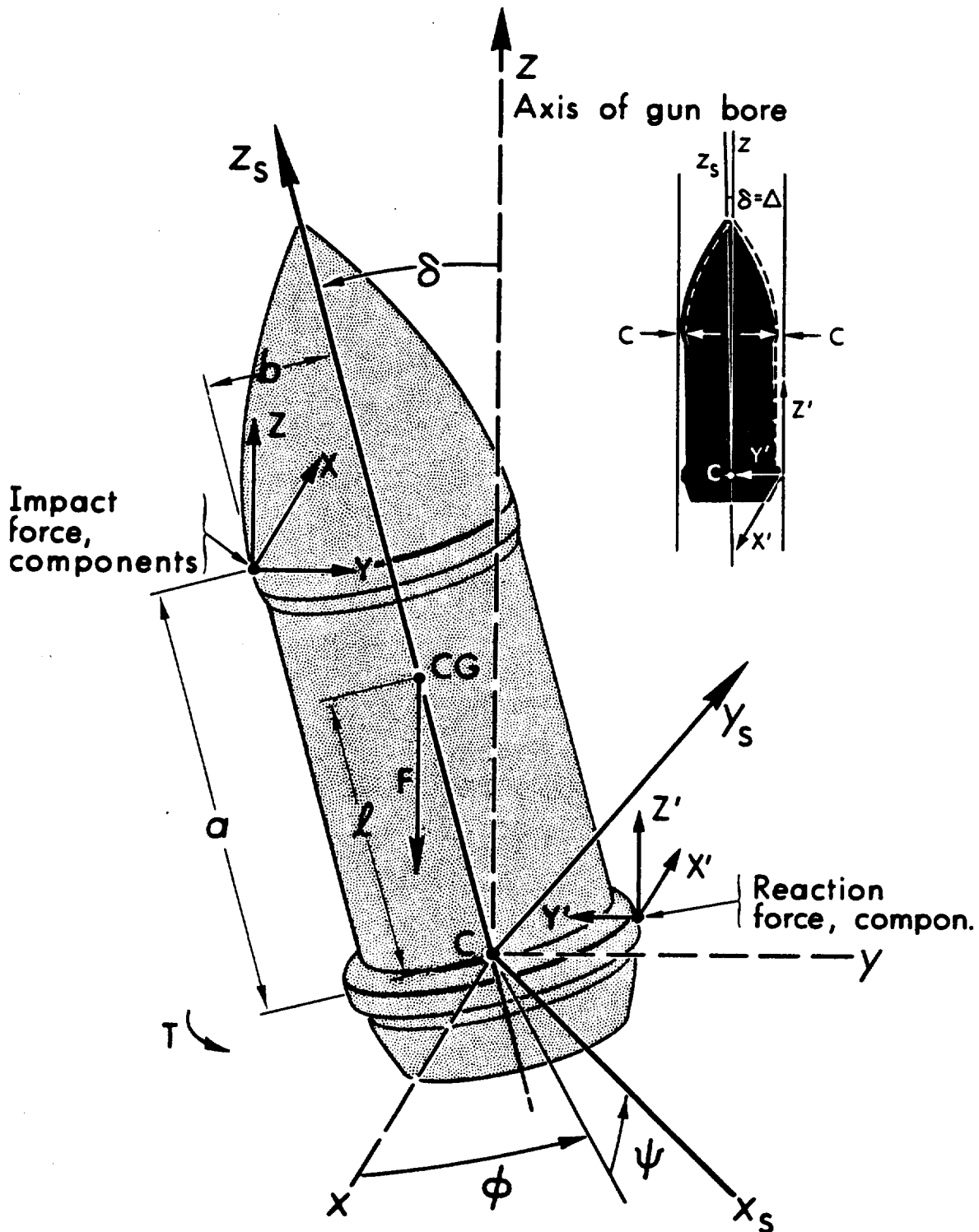


Figure 1. Euler's angles, δ , ϕ , ψ , specifying the orientation of a symmetrical shell about a point C at the center of the rotating band on the shell axis. The accelerating force F , and the components of the impact forces acting on the bourrelet X , Y , Z , and the reaction forces on rotating band X' , Y' , Z' are indicated together with the driving torque on the rotating band due to the rifling of the tube. The yaw angle δ is greatly exaggerated. Also shown are the dimensions a , the distance between the rotating band and bourrelet, l , the distance from C to the center of gravity, CG , and b , the radius at the bourrelet. The insert shows the clearance c at the bourrelet and the reaction forces at the rotating band.

and the Q_i are the generalized forces in the respective directions;

$$Q_1 d\delta = [Y(a \cos \delta - b \sin \delta) - Z(a \sin \delta + b \cos \delta) + Z'r]d\delta \quad (8)$$

where the moment arm of Y' has been taken to be zero. If the rotating band does not deform into a section of a sphere of radius r but remains a plane, $Z'r$ should be replaced by $Y'b' \sin \delta + Z'b' \cos \delta$ where b' is the distance between c and the point of "center of contact" between the rotating band and the bore ("center of contact" refers to the point at which the effective or equivalent of the forces acting on the rotating band originates). In the ϕ direction

$$Q_2 d\phi = [-X(a \sin \delta + b \cos \delta) + X'r \cos \delta]d\phi \quad (9)$$

and

$$Q_3 d\psi = [-Xb + X'r + T]d\psi, \quad (10)$$

where T is the torque on the rotating bands as such, not arising from impact action and reaction forces.

Equations (3) through (10) yield

$$\begin{aligned} I\ddot{\delta} - I\dot{\phi}^2 \sin \delta \cos \delta + A(\dot{\psi} + \dot{\phi} \cos \delta)\dot{\phi} \sin \delta - m\ddot{s} \ell \sin \delta &= Q_1 \\ &= (a \cos \delta - b \sin \delta)Y - (a \sin \delta + b \cos \delta)Z + rZ' \end{aligned} \quad (11)$$

$$\begin{aligned} \frac{d}{dt} [I\dot{\phi} \sin^2 \delta + A(\dot{\psi} + \dot{\phi} \cos \delta)\cos \delta] &= Q_2 \\ &= -(a \sin \delta + b \cos \delta)X + r \cos \delta X' + T \cos \delta \end{aligned} \quad (12)$$

$$\frac{d}{dt} [A(\dot{\psi} + \dot{\phi} \cos \delta)] = Q_3 = -bX + rX' + T. \quad (13)$$

Before proceeding, it will be appropriate to compare Equations (11-13) with the expressions derived by Thomas. According to the assumptions made by Thomas, when $\delta < \Delta$, the forces Q_1 , Q_2 , and Q_3 were set equal to zero. Under these assumptions, Equations (11-13) yield

$$I\ddot{\delta} - I\dot{\phi}^2 \sin \delta \cos \delta + A(\dot{\psi} + \dot{\phi} \cos \delta)\dot{\phi} \sin \delta - m\ddot{s} \ell \sin \delta = 0, \quad (14)$$

$$I\dot{\phi} \sin^2 \delta + A(\dot{\psi} + \dot{\phi} \cos \delta) \cos \delta = C_1, \quad (15)$$

$$\dot{\psi} + \dot{\phi} \cos \delta = C_2, \quad (16)$$

where C_1 and C_2 are integration constants. Equations (14) and (15) are identical to those of Thomas, while for (16) Thomas gives

$$\dot{\psi} + \dot{\phi} = \dot{\alpha}, \quad (17)$$

where $\alpha = \pi s/nr$; here n is the twist of the rifling in calibers/turn. Since $\cos \delta$ is, for all practical purposes, equal to unity, the difference between the left-hand sides of Equations (16) and (17) is not important. However, the right-hand side of (17) is not a constant. As a consequence, (17) is not satisfactory under the assumptions made by Thomas.

Under all conditions of the motion of the projectile (where the lands and rotating band are intact), the torque on the rotating band due to forces on the band from the groove walls (see Figure 2 where these forces are indicated by X_i^*) acts at all times to constrain the value of ψ so that

$$\dot{\psi} = \frac{\pi \dot{s}}{rn} \equiv \Omega(s), \quad (18)$$

where \dot{s} is the velocity of the point C (at the center of the rotating band on the projectile axis) along the gun tube axis. Except for the initial deformation of the rotating band, the band does not constrain $\dot{\phi}$.

Under the conditions of no impact or reaction forces, therefore, we obtain, substituting for (18) in Equations (11), (12), and (13) and setting all the impact and reaction forces to zero,

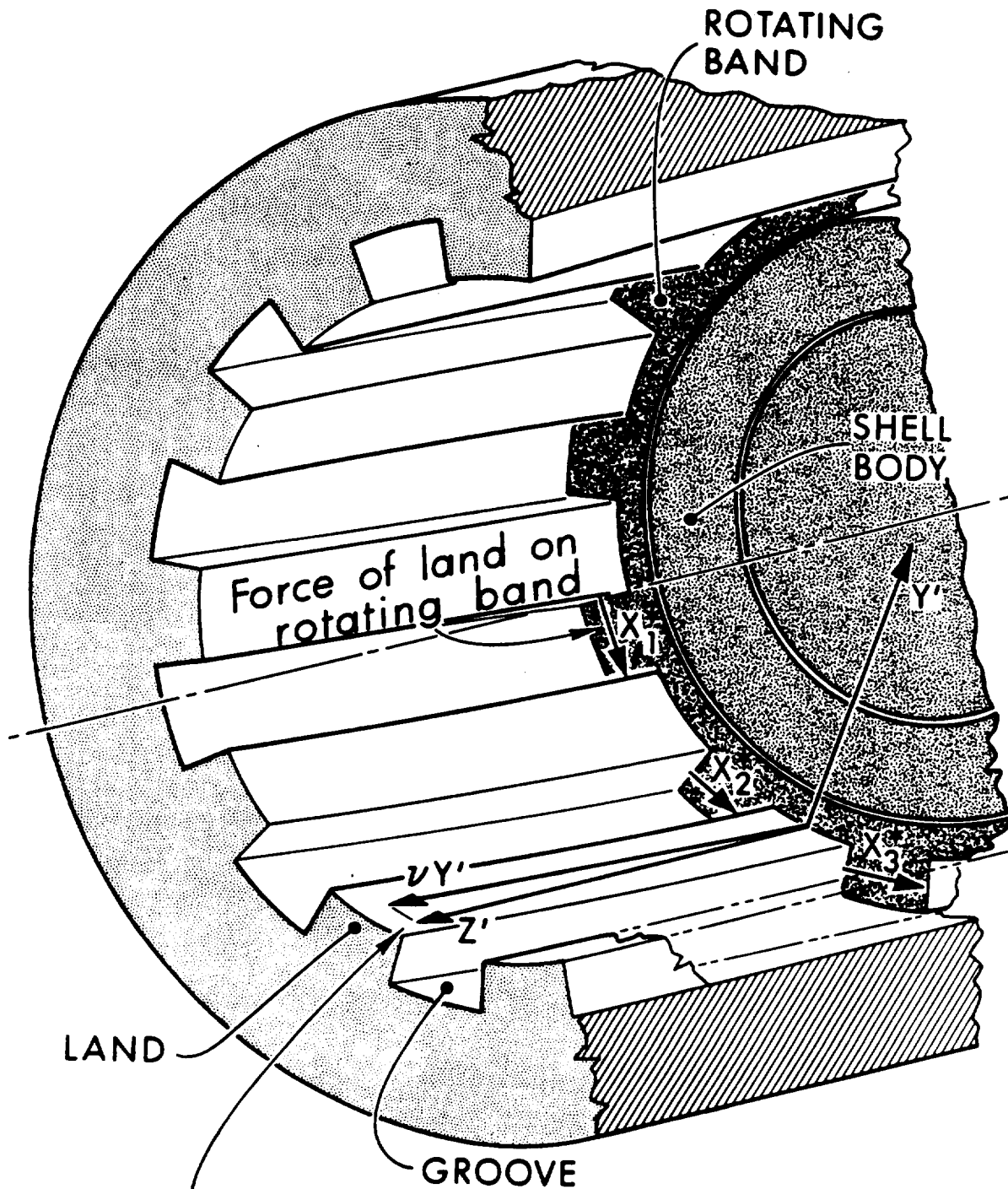
$$I\ddot{\delta} - I\dot{\phi}^2 \sin \delta \cos \delta + A(\Omega + \dot{\phi} \cos \delta)\dot{\phi} \sin \delta - m\ddot{s} \ell \sin \delta = 0, \quad (19)$$

$$I\dot{\phi} \sin^2 \delta + A(\Omega + \dot{\phi} \cos \delta) \cos \delta = \cos \delta \int T dt, \quad (20)$$

$$A(\Omega + \dot{\phi} \cos \delta) = \int T dt. \quad (21)$$

If we eliminate the integral over T from Equations (20 and 21), we obtain, repeating from above to give the full set of equations,

$$(I\ddot{\delta} - I\dot{\phi}^2 \sin \delta \cos \delta - m\ddot{s} \ell \sin \delta)\dot{\delta} + \dot{\phi} \frac{d}{dt} (I\dot{\phi} \sin^2 \delta) = 0, \quad (22)$$



Z' , component of frictional force
in z direction

Figure 2. Sketch of the region of contact between the gun tube bore and the rotating band of a shell. The forces X_1^* , X_2^* , X_3^* ... acting through the moment arm r give rise to the torque T' : $T' = r \sum_i X_i^*$. Balloting impacts give rise to a force Y' at the rotating band, friction results in the force vY' having a component in the direction of travel of the shell (parallel to the bore axis), Z' .

$$\frac{d}{dt} (I\dot{\phi} \sin^2 \delta) - A(\Omega + \dot{\phi} \cos \delta) \sin \delta \dot{\delta} = 0, \quad (23)$$

$$\Omega = \pi \dot{s} / r_n, \quad (24)$$

and

$$T = \frac{d}{dt} [A(\Omega + \dot{\phi} \cos \delta)]. \quad (25)$$

This last equation can be used to determine the forces tending to shear the lands along planes parallel to the top of the lands.

Equations (22) and (23) can be put in an interesting and simple form, although one that is not solvable in closed form,

$$\ddot{\delta} / \sin \delta = S - \Omega' \dot{\phi} - I' \dot{\phi}^2 \cos \delta, \quad (26)$$

where

$$I' = \frac{A}{I} - 1, \quad (27)$$

$$\Omega' = A\Omega / I, \quad (28)$$

and

$$S = m\ddot{s}\ell / I. \quad (29)$$

If we multiply Equation (26) through by I , the $\dot{\phi}^2$ term will be of the order of (but not equal to) the kinetic energy in the precession motion, the term in Ω' will be of the order of the spin kinetic energy reduced by a factor ϕ/Ω and S will be the increase in the kinetic energy of the projectile in traveling a distance ℓ . Now the kinetic energy E_ψ in the spin of the projectile in terms of k_a , the radius of gyration about the shell axis and the translational kinetic energy E_s , is

$$E_\psi = \frac{1}{2} A\Omega^2 = E_s (k_a \pi / r_n)^2. \quad (30)$$

Thus, in terms of an effective length of the gun L_e as would be required to achieve the shell translational energy E_s at a constant force of $m\ddot{s}$,

$$\frac{\Omega' \dot{\phi}}{S} = \frac{2L_e \dot{\phi}}{\ell \Omega} \left(\frac{k_a \pi}{r_n} \right)^2. \quad (31)$$

Since for much of the projectile travel n^2 is much larger than L_e/ℓ , the term S dominates the right side of Equation (26). Assuming S is

constant during the swing of projectile from the axis to the gun tube wall and $\sin \delta \approx \delta$, we obtain the approximate expression

$$\ddot{\delta} = S \sin \delta \quad (32)$$

having a solution for $\dot{\delta} = \dot{\delta}_0$ and $\delta = 0$ at $t = 0$,

$$\delta = \frac{\dot{\delta}_0}{2\sqrt{S}} \left(e^{\sqrt{S}t} - e^{-\sqrt{S}t} \right) \quad (33)$$

With this function determined and substituted into Equation (26), it is possible to obtain an approximate solution for ϕ . However, such solutions are of limited value in the practical case in which the principal characteristics of the motion are due to the impacts and the reaction forces acting on the rotating band.

Let us now turn to the expressions for the forces and torques acting on the shell in the general case which includes impacts and reaction forces. The Hertz⁵ theory of impact can be employed advantageously to obtain a good expression for Y acting during impact together with Raman's⁶ formulas for the coefficient of restitution. Gay's expression for Y is

$$Y = \begin{cases} -K_c(\delta - \Delta), & \dot{\delta} > 0 \\ -K_r(\delta - \Delta), & \dot{\delta} < 0 \end{cases} \quad \delta > \Delta \quad (34)$$

$$0, \quad \delta \leq \Delta$$

for which the coefficient of restitution e can be expressed as

$$e = (K_r/K_c)^{1/2}. \quad (35)$$

The X and Z forces are dependent on the coefficient of friction μ and on the direction of motion* of the point on the bourrelet in contact with the gun tube. We have, after Thomas (Reference 2)

$$X^2 + Z^2 = \mu^2 Y^2 \quad (36)$$

* that is, the sign of $\dot{\delta}$.

and

$$\frac{X}{b(\dot{\Omega} + \dot{\phi} \cos \delta) + a\dot{\phi} \sin \delta} = \frac{Z}{\dot{s}} \quad (37)$$

or as an approximation,

$$X \approx Zb\dot{\Omega}/\dot{s}. \quad (38)$$

The force component Y' is given by the requirement that the sum of the forces acting in the y direction must be zero. However, since the shell is elastic (i.e., not infinitely rigid), there will be a time lag τ_e between the application of the forces Y and Y' to the shell. Thus we have that

$$Y'(t) = -Y(t - \tau_e) \quad (39)$$

where we can evaluate τ_e approximately, in terms of the shear wave velocity c_s in the shell, using the expression

$$\tau_e = \sqrt{\pi^2 b^2 + a^2}/c_s. \quad (40)$$

The frictional reaction forces X' and Z' are given in terms of the coefficient of friction ν between the rotating band and the tube wall by

$$X'^2 + Z'^2 = \nu^2 Y'^2 \quad (41)$$

and the relation for the ratio of X' to Z' in terms of velocity components

$$X' = Z' r\dot{\Omega}/\dot{s} \quad (42)$$

which, on substitution into Equation (41), yields

$$Z' = \nu Y' / \sqrt{1 + (r\dot{\Omega}/\dot{s})^2}. \quad (43)$$

The total torque $T' = Q_3$ acting in the z direction [i.e., the right-hand side of Equation (13)] is constrained by the requirement that

$$\dot{\psi} = \Omega = \pi \dot{s}/r\pi \quad (44)$$

as previously given. Thus we have that

$$T' = T + rX' - bX = \frac{d}{dt} [A(\Omega + \dot{\phi} \cos \delta)] \quad (45)$$

which, as mentioned above, can be evaluated in terms of the solution to the general problem to determine the shears acting across the lands.

The Equations (11-13), (34-37), and (39-45) provide the complete set of equations for computing the balloting of the shell where the function $s(t)$ is given. A calculation of this motion will be presented in a separate paper. The following treatment is carried out to show the importance of these reaction forces.

III. GROWTH OF ENERGY IN THE TRANSVERSE MODE

The motion of the projectile in the bore of the gun that can lead to severe impact by the bourrelet against the lands is the motion along the δ coordinate. We will now develop the equations describing the growth in energy in this transverse motion about the point C (Figure 1) by first calculating the effects due to bourrelet impact against the lands and the subsequent reaction torques applied at the rotating band and then express this in the form of a time-averaged equation for this energy.

If during the time $t = 0$ to $t = t_1$ the shell moves $\delta = \Delta$ (i.e., bourrelet just making contact with the lands) to $\delta = \delta_{\max}$ where $\dot{\delta} = 0$ as a result of the impact and if t_2 is the total duration of the contact between the bourrelet and the lands for the impact, we can write, integrating over Equation (11) for $t = 0$ to Δt , the time between impacts of the bourrelet with the lands

$$\int_0^{\Delta t} [I\ddot{\delta} - I\dot{\phi}^2 \sin \delta \cos \delta + A(\Omega + \dot{\phi} \cos \delta)\dot{\phi} \sin \delta - m\ddot{s} \ell \sin \delta] dt \quad (46)$$

$$= \int_0^{t_2} [(a \cos \delta - b \sin \delta)Y - (a \sin \delta + b \cos \delta)Z] dt + \int_{\tau_e}^{\tau_e + t_2} rZ' dt$$

where Z' is zero during the interval $\tau_e < t < \tau_e + t_2$ and Y and Z are zero for $t_2 < t < \Delta t$,

Let us first show that the second and third terms on the left side of Equation (46) do not contribute significantly to the motion computed during the impacts. We have from Equations (13) and (18)

$$\frac{d}{dt} [A(\Omega + \dot{\phi} \cos \delta)] = -bX + rX' + T \quad (47)$$

where from Equations (18), (36), (38), (42), and (43)

$$X = \mu Y / \sqrt{1 + \frac{r^2 n^2}{b^2 \pi^2}} \quad (48)$$

and

$$X' = \nu Y' / \sqrt{1 + n^2/\pi^2}. \quad (49)$$

Since

$$b \approx r \quad (50)$$

we can write, using Equation (39) to obtain a result holding for a single cycle of the motion (that is to say, the action and reaction impulses)

$$\dot{\phi} \frac{d}{d\phi} [A(\Omega + \dot{\phi} \cos \delta)] \approx r \frac{\mu Y(t) - \nu Y(t - \tau_e)}{\sqrt{1 + n^2/\pi^2}} + T. \quad (51)$$

Noting that the change in δ is extremely small during each impact we have, integrating (51) twice,

$$\begin{aligned} & \int_0^{t_2} [A(\Omega + \dot{\phi} \cos \delta) \dot{\phi} \sin \delta] dt + \int_{\tau_e}^{\tau_e + t_2} [A(\Omega + \dot{\phi} \cos \delta) \dot{\phi} \sin \delta] dt \\ & \approx \frac{\mu \Delta - \nu \delta'}{\sqrt{1 + n^2/\pi^2}} r \bar{Y} (\Delta \phi) t_2 + (\Delta + \delta') T \Delta \phi \cdot t_2 \end{aligned} \quad (52)$$

where δ' is the value of δ at $t = \tau_e + t_1$, $\Delta \phi$ is the equivalent angle that the shell moves through during the interval t_2 and \bar{Y} is the average force applied in the y direction. Now subtracting Equation (13) from (12) gives

$$\begin{aligned}
& \frac{d}{dt} [I \dot{\phi} \sin^2 \delta + A(\Omega + \dot{\phi} \cos \delta) (\cos \delta - 1)] \\
& = (b - b \cos \delta - a \sin \delta) X + (\cos \delta - 1) r X' \\
& \quad + (\cos \delta - 1) T.
\end{aligned} \tag{53}$$

Repeating the above procedure gives

$$\begin{aligned}
& \int_0^{t_2} [I \dot{\phi}^2 \sin \delta \cos \delta + A(\Omega + \dot{\phi} \cos \delta) \dot{\phi} \sin \delta] dt \\
& + \int_{\tau_e}^{\tau_e+t_2} [I \dot{\phi}^2 \sin \delta \cos \delta + A(\Omega + \dot{\phi} \cos \delta) \dot{\phi} \sin \delta] dt \\
& \approx [(b \Delta - a) \mu + r \delta' \nu] \frac{\bar{Y} \Delta \phi \cdot t_2}{\sqrt{1 + n^2/\pi^2}} + (\Delta + \delta') T t_2 \Delta \phi.
\end{aligned} \tag{54}$$

Thus from (52) and (54) we have

$$\begin{aligned}
& \int_0^{t_2} [-I \dot{\phi} \sin \delta \cos \delta + A(\Omega + \dot{\phi} \cos \delta) \dot{\phi} \sin \delta] dt \\
& + \int_{\tau_e}^{\tau_e+t_2} [-I \dot{\phi}^2 \sin \delta \cos \delta + A(\Omega + \dot{\phi} \cos \delta) \dot{\phi} \sin \delta] dt \\
& \approx \left[\frac{(\mu \Delta - \nu \delta' + \mu a)}{\sqrt{1 + n^2/\pi^2}} \bar{Y} + (\Delta + \delta') T \right] t_2 \Delta \phi \\
& \approx \frac{\mu a \bar{Y} t_2 \Delta \phi}{\sqrt{1 + n^2/\pi^2}}.
\end{aligned} \tag{55}$$

We will find below that this contribution is smaller than other terms by

a factor $\Delta\phi / \sqrt{1 + n^2/\pi^2}$ where $\Delta\phi$ is the angle through which the shell precesses during the impact of the bourrelet.

Returning again to Equation (46) we see that for complete cycles of the motion for which δ varies between $\pm \delta_{\max}$, the second, third and fourth terms contribute no time averaged change to the motion (although these terms do effect the value of Δt) since $\sin \delta$ changes sign for negative values of δ . This cannot be stated if δ always satisfies

$$\delta > 0 , \quad (56)$$

in which a more detailed calculation using numerical techniques is required. The condition in (56) will occur if no significant initial balloting occurs. Under such conditions it is expected that bore riding will be a likely mode of projectile motion in the bore.

Making use of Equations (18), (36), (38) and (44) and setting

$$a \cos \delta - b \sin \delta \approx a \quad (57)$$

$$a \sin \delta + b \cos \delta \approx b \quad (58)$$

and $r \approx b . \quad (59)$

Equation (46) in the time interval $0 \leq t \leq t_2$ becomes

$$\left[a - b \mu / \sqrt{1 + \pi^2/n^2} \right] \int_0^{t_2} Y dt = I \int_0^{t_2} \delta dt . \quad (60)$$

Now the coefficient of restitution may be more generally defined than as given in Equation (35). In general we have

$$\int_0^{t_1} Y dt = \left(2I \int_{\Delta}^{\delta_{\max}} Y d\delta \right)^{1/2} = \left(2I \int_{\Delta}^{\delta_{\max}} f_1(\delta) d\delta \right)^{1/2} \quad (61)$$

while

$$\int_{t_1}^{t_2} Y dt = \left(2I \int_{\delta_{\max}}^{\Delta} f_2(\delta) d\delta \right)^{1/2} = e \left(2I \int_{\Delta}^{\delta_{\max}} f_1(\delta) d\delta \right)^{1/2} . \quad (62)$$

As a result, Equation (61) multiplied through by the moment arm

$[a - b \mu / \sqrt{1 + \pi^2/n^2}]$ gives the loss in angular momentum as the shell momentarily stops while Equation (62) multiplied through by this moment arm gives an expression for the recovered angular momentum. Thus Equation (60) gives us

$$\left[a - b \mu / \sqrt{1 + \pi^2/n^2} \right] \int_0^{t_2} Y dt = - (1 - e) I \dot{\delta}_i \quad (63)$$

where $\dot{\delta}_i$ is the angular velocity at impact. This can also be expressed in terms of an average torque \bar{T}_y acting for the time interval Δt between impacts:

$$\bar{T}_y \Delta t = (e - 1) I \dot{\delta}_i . \quad (64)$$

The last term in Equation (46) is the integral over the torque rZ' . If

$$t_2 \leq \tau_e \leq \Delta t \quad (65)$$

then both the direction of the torque and the displacement of the shell in the δ direction will retain their signs unchanged during the interval $t = \tau_e$ to $\tau_e + t_2$. It was the change in directions of motion that gave rise to the sign change resulting in the factor $(1-e)$ in Equation (63). The rZ' torque accelerates the angular motion of the shell in the δ direction throughout the time interval τ_e to $\tau_e + t_2$. During this time interval Y and Z will be zero. We have, therefore,

$$r \int_{\tau_e}^{\tau_e+t_2} Z' dt = I \int_{\tau_e}^{\tau_e+t_2} \ddot{\delta} dt . \quad (66)$$

From Equations (39), (43) and (44) we have

$$Z'(t) = - v Y(t - \tau_e) / \sqrt{1 + \pi^2/n^2} . \quad (67)$$

Thus, the time average torque \bar{T}_z will be

$$\begin{aligned} \bar{T}_z \Delta t &= r \int_{\tau_e}^{\tau_e+t_2} z' dt = - \frac{vr}{\sqrt{1 + \pi^2/n^2}} \int_0^{t_2} Y dt \\ &= \frac{(1+e) v r I \dot{\delta}_i}{a \sqrt{1 + \pi^2/n^2} - \mu b} = I \int_{\tau_e}^{\tau_e+t_2} \ddot{\delta} dt. \end{aligned} \quad (68)$$

Now let us introduce a quantity Θ defined by

$$\Theta(t) = \int_0^t |\dot{\delta}| dt \quad (69)$$

which is simply the total angle swept out by the shell in the δ direction, ignoring the direction of motion. Introducing this angle allows us to treat the impacts between the bourrelet and the bore in a time averaged way. From Equations (46), (64), (68) and (69) we have

$$I \ddot{\Theta} = \left[\frac{(1+e) v r}{a \sqrt{1 + \pi^2/n^2} - \mu b} + (e-1) \right] \frac{I \dot{\Theta}}{\Delta t}. \quad (70)$$

An expression for Δt can be obtained using Equation (33). Expanding Equation (33) in a series gives

$$\delta = \frac{\dot{\delta}_0}{2\sqrt{S}} (2\sqrt{S} t + \dots) \quad (71)$$

where $\dot{\delta}_0$ is the angular velocity at $\delta = 0$. If $\frac{1}{2} S \Delta t \ll 1$ we can write for a swing through an angle 2Δ :

$$\Delta t = 2\Delta/\dot{\delta}_0. \quad (72)$$

If we let c be the clearance on each side of the bourrelet then

$$\Delta = c/a \quad (73)$$

and

$$\Delta t = 2c/a\dot{\theta} . \quad (74)$$

Substituting Equation (74) into (70) and writing

$$\epsilon = \frac{1}{2} I \dot{\theta}^2 \quad (75)$$

gives, if $t_2 < \tau_e < \Delta t$,

$$\frac{d\epsilon}{d\theta} = \gamma\epsilon \quad (76)$$

where

$$\gamma = \frac{a}{c} \left[\frac{(1+e) v r}{a \sqrt{1 + \pi^2/n^2} - \mu b} + (e-1) \right] . \quad (77)$$

For an initial energy of $\epsilon = \epsilon_0$ at $\theta = 0$, $t = 0$, integration of Equation (76) gives

$$\epsilon = \epsilon_0 e^{\gamma\theta} . \quad (78)$$

This can also be integrated a second time to yield

$$t = \frac{1}{\gamma} \sqrt{\frac{2I}{\epsilon_0}} \left(1 - e^{-\gamma\theta/2} \right) = \frac{1}{\gamma} \sqrt{\frac{2I}{\epsilon_0}} \left(1 - \sqrt{\epsilon_0/\epsilon} \right) \quad (79)$$

or, more conveniently,

$$\epsilon = \epsilon_0 / (1 - \sqrt{\epsilon_0/2I} \gamma t)^2 . \quad (80)$$

This growth in the energy in the transverse mode requires that several conditions be met:

$$(i) \quad \gamma > 0 \quad (81)$$

$$(ii) \quad \tau_e > t_2 \quad (82)$$

$$(iii) \quad \tau_e < 2c/a\dot{\theta} \text{ for all } \dot{\theta} \quad (83)$$

$$(iv) \quad \epsilon_0 > 0. \quad (84)$$

Condition (iv) implies that some additional mechanism must initiate the balloting motion. Clearly balloting, particularly the development of violent balloting, is not to be expected in all cases. However, once this motion is initiated, the energy of the system rapidly moves into this mode. Figure 3 shows how this energy increases with motion of the projectile down the gun tube until some damage to the shell or to the bore removes the energy. Subsequently, the energy in this motion again increases until the shell exits or general failure occurs.

IV. INITIAL MOTION OF THE PROJECTILE

To calculate the growth of energy in the transverse mode using Equation (80), it is necessary to calculate the initial energy ϵ_0 in that mode. That energy comes from the initial swing of the shell. Since initially ϕ , Y , Z and Z' are all zero, Equation (11) gives

$$I \ddot{\delta} = \frac{d\epsilon}{d\delta} = m \ddot{s} \ell \sin(\delta + \delta_c) \quad (85)$$

where δ_c designates the angle between the shell axis and the center of gravity projected on the y - z plane. For cases in which the \ddot{s} can be treated as constant we have, taking $\epsilon = 0$, $\delta = 0$ at $t = 0$:

$$\begin{aligned} \epsilon_0 &= m \ddot{s} \ell (1 - \cos \Delta) \\ &\approx m \ddot{s} \ell c^2/2 a^2. \end{aligned} \quad (86)$$

In general, this is not the case however. It is necessary to take account of the change in pressure as a function of time, requiring numerical methods.

It will be noticed that unless the initial value of the center of gravity yaw, $\delta_0 + \delta_c$, differs from zero, there will be no motion in the δ direction.

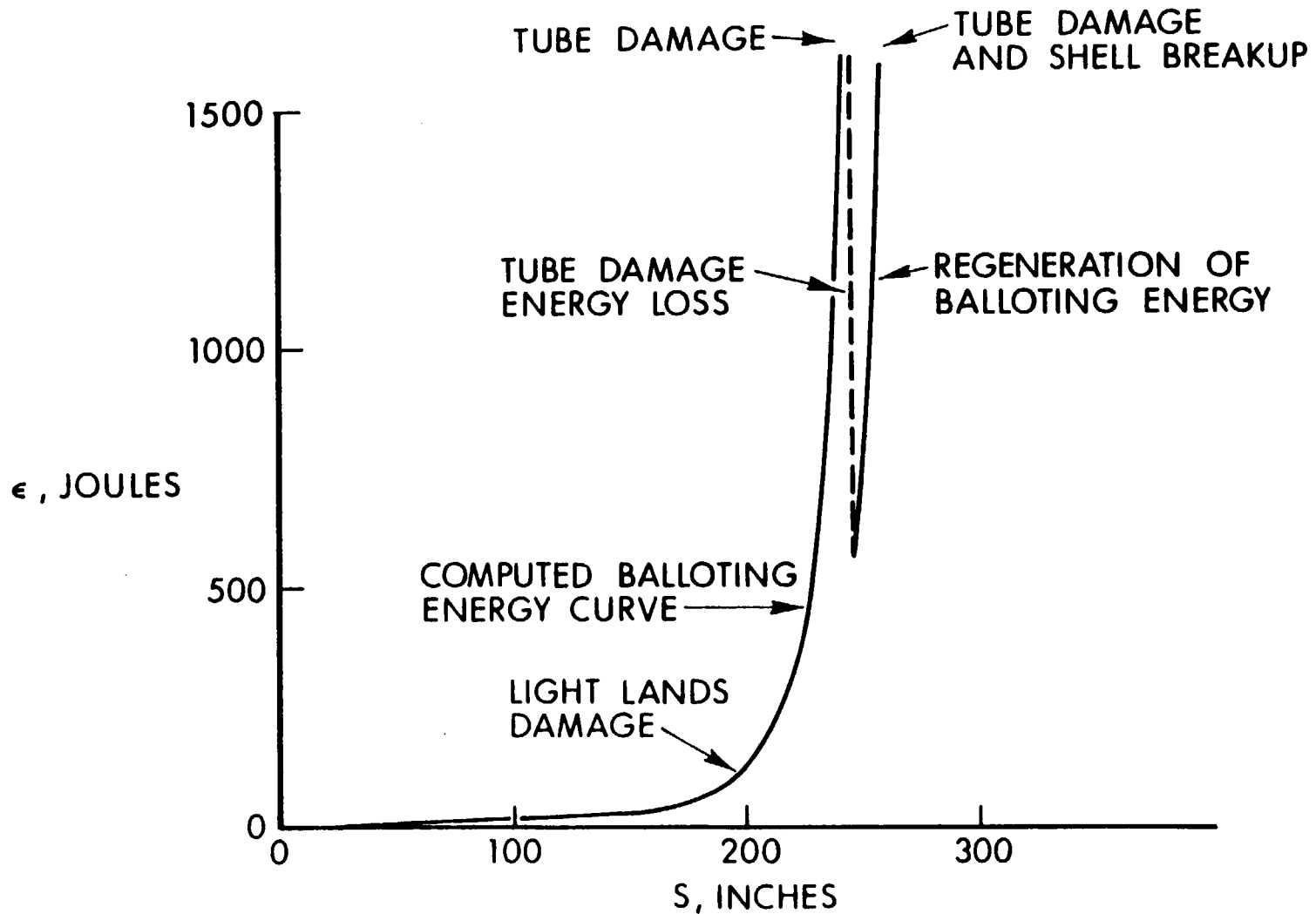


Figure 3. Calculation of balloting energy ϵ as a function of shell position s in the 8" Howitzer tube for a zone 9 charge as computed using Eq. (80) and the results of the integration of Eq. (85). Values of constants used are as given in the text with $I = 5.245$ slug ft² and $\gamma = 140.6$. The energy rapidly rises probably producing the first bands damage (see Para. a, Section VI) without significant loss in energy. The major damage (see Para b, Section VI) would remove a significant amount of the balloting energy as indicated by the dashed line. Regeneration of balloting would lead to further tube damage (see Para c, Section VI).

The closer $\delta_o + \delta_c$ is to zero initially the longer will be the time until the shell bourrelet strikes the bore wall. This delay allows the pressure and thus \dot{s} to increase. The likelihood that δ_o will be sufficiently small to allow for a sufficient delay in this impact is small and largely determines the probability that ϵ_o will be sufficiently large to cause significant balloting.

Figure 4 shows the results of numerical integration of Equation (85) for the conditions of an 8" M106 HE shell launched with a zone 9 charge producing a pressure history as given in Figure 5. The shell parameters as used here were:

$$\begin{aligned} \text{weight } mg &= 201. \text{ lbs} \\ I &= 5.245 \text{ slug ft}^2 \\ c &= 0.0142'' \\ a &= 9.08'' \\ l &= 5.678''. \end{aligned}$$

In addition, Figure 4 together with the results in Figure 6 gives the probability that the initial value of $\delta = \delta_o$ will lead to gun damage assuming all possible initial positions are equally likely. The probability P is given by the ratio of solid angles giving rise to sufficient energy to cause damage Ω_d divided by the total solid angle allowed for the initial shell position:

$$P = \Omega_d / \pi \Delta^2 . \quad (87)$$

Since t in Equation (80) will be a function of δ_o one must compute ϵ and evaluate Equation (87). This result is shown in Figure 6.

V. CALCULATION OF THE COEFFICIENT OF RESTITUTION

An examination of Equations (77) and (81) shows that the coefficient of restitution is an important parameter of balloting motion. Accurate calculations of this motion properly requires an experimental determination of this parameter for the particular conditions of the shell in the bore. An approximation to the value can be obtained, nevertheless by adopting the formulas for the coefficient of restitution developed by Raman⁶ which were based on Hertz's⁵ (see also the treatise on elasticity by Love⁷) theory of impact.

From Hertz's Theory we have for the duration of an impact between two spheres of radii r_1 and r_2 :

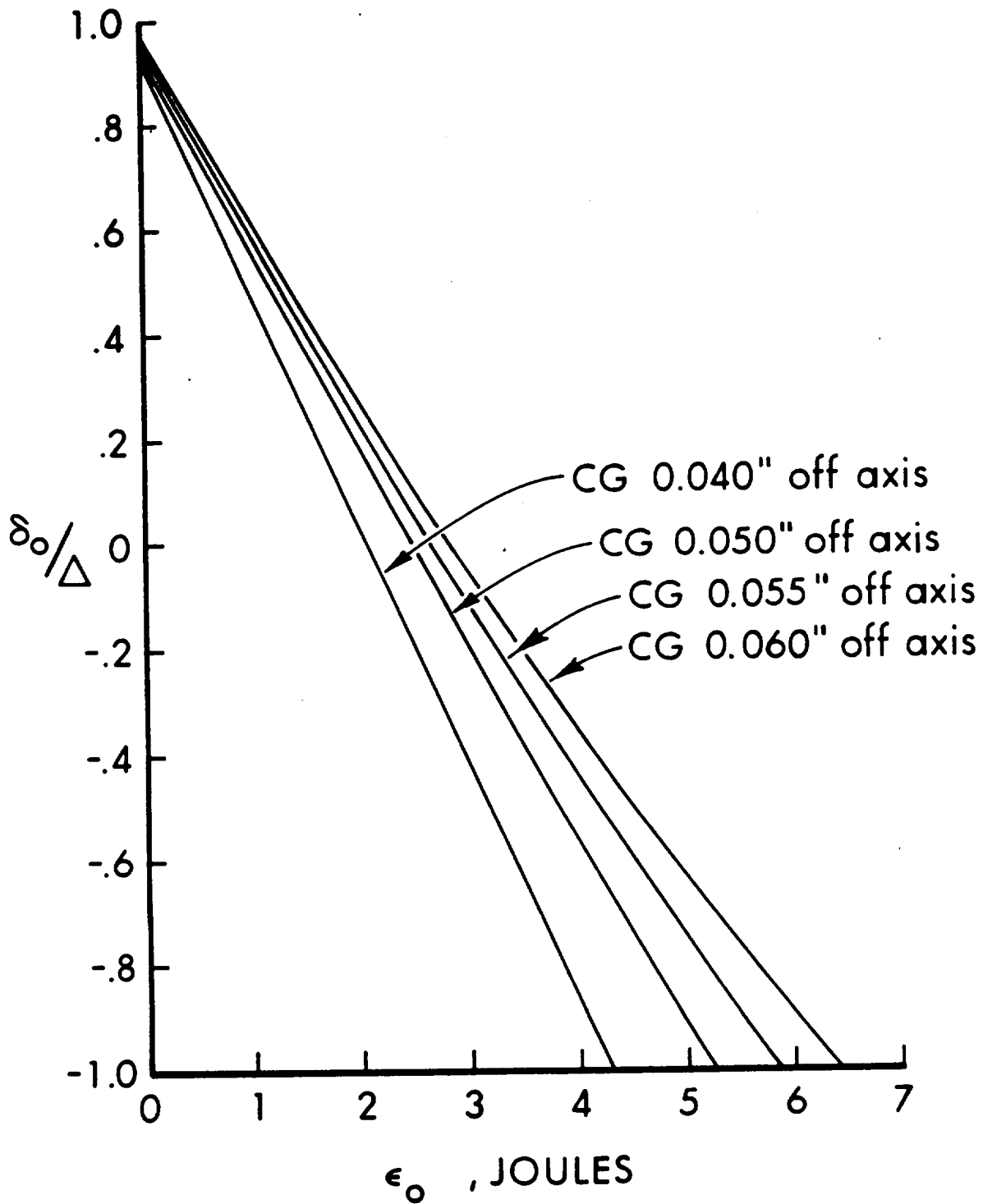


Figure 4. Plot of the energy ϵ_0 in the balloting mode at first impact with the gun bore as a function initial shell altitude (yaw angle δ_0 divided by the maximum yaw angle Δ) as computed from Eq. (85) for the 8" M106 HE shell launched with a zero 9 charge in the XM201 Howitzer tube. The pressure history used for these calculations is given in Figure 5.

CHARGE at -70°F

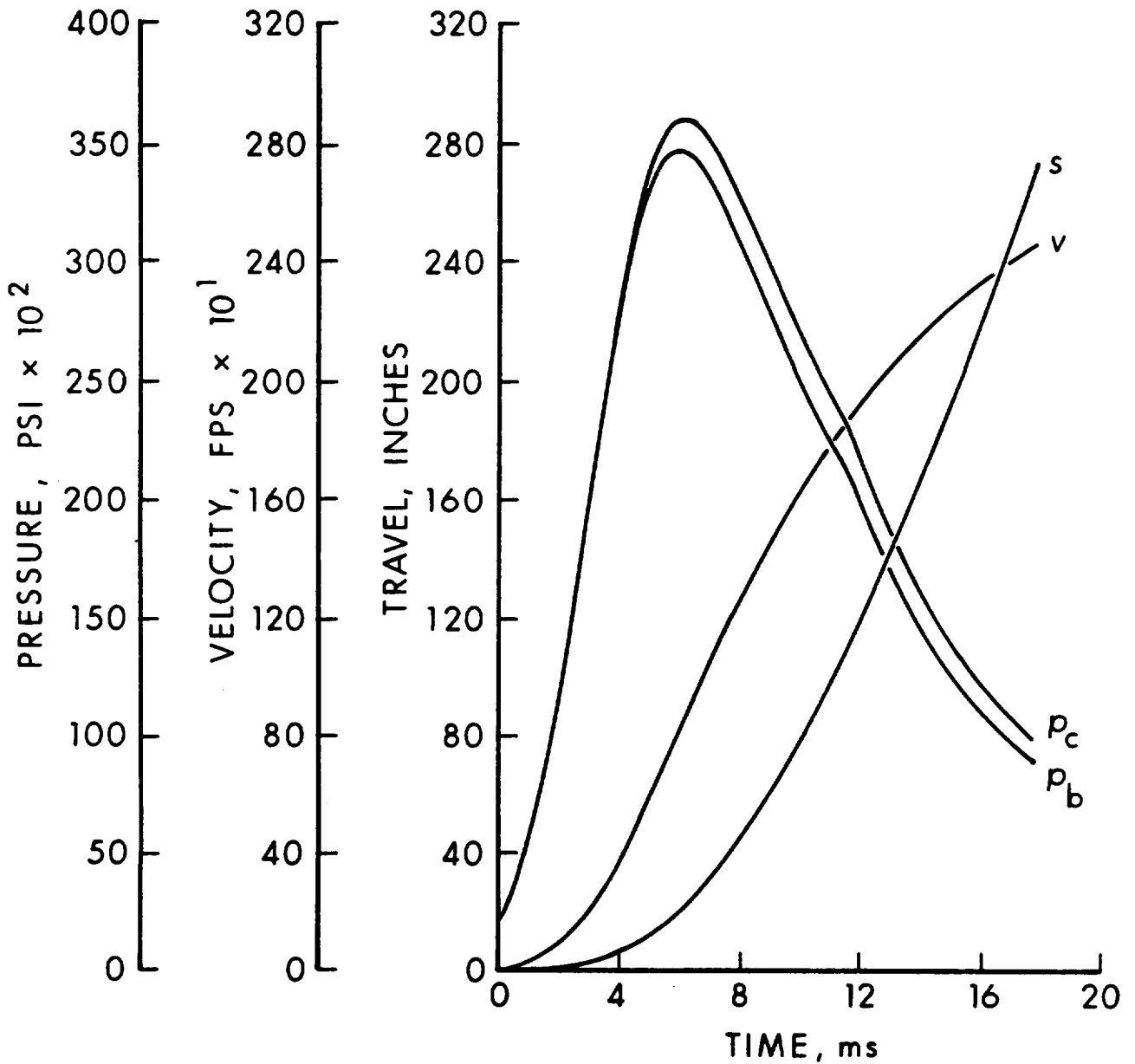


Figure 5. Plot of the pressure time curves computed by L.D. Heppner of MTD for the 8" M106 HE shell launched with an XM188 zone 9 charge at -70°F in the XM201 Howitzer tube. The chamber pressure p_c , base pressure p_b , velocity v and position z of the shell in the tube are shown. These curves were used to compute the results given in Figures 4 and 6.

$$t_2 = 2.94 \left[\frac{15}{16} \left(\frac{1 - \sigma_1^2}{q_1} + \frac{1 - \sigma_2^2}{q_2} \right) \frac{m_1 m_2}{m_1 + m_2} \right]^{2/5} \left[\frac{1}{v} \left(\frac{r_1 + r_2}{r_1 r_2} \right) \right]^{1/5} \quad (88)$$

where

σ_1, σ_2 = The Poisson's ratio for the first and second ball, respectively.

q_1, q_2 = The Young's modulus for the first and second ball, respectively.

m_1, m_2 = mass of the first and second impacting ball, respectively.

v = velocity of impact.

Raman modified Equation (88) to apply to the case of a ball of mass m_2 impacting against a plate of thickness $2b_1$ and density ρ_1 obtaining

$$e = \frac{b_1 \rho_1 a^2 - \kappa m_2}{b_1 \rho_1 a^2 + \kappa m_2} \quad (89)$$

where κ is a coefficient describing the dominant vibrational mode, a^2 is

$$a^2 = \pi t_2 b_1 \sqrt{q_1 / 3 \rho_1 (1 - \sigma_1^2)} \quad (90)$$

and where Raman has taken the approximations

$$m = m_2 \approx \frac{m_1 m_2}{m_1 + m_2} \quad (91)$$

and

$$r_2 \approx \frac{r_1 r_2}{r_1 + r_2} \quad (92)$$

Raman gives values of $\kappa = 0.56, 0.44$ and 0.39 .

Because of the special geometry with which we are dealing in the case of a shell bourrelet impacting against the gun tube wall, we will also assume Equation (91) holds and replace the term $r_1 r_2 / (r_1 + r_2)$ by

$$\xi \sqrt{l_b \left(\frac{r_1 r_2}{r_1 - r_2} \right)} \quad (93)$$

where ξ is the portion of the gun tube lands to lands plus grooves area and ℓ_b is the radius of curvature of the bourrelet contacting the lands. The expression in Equation (93) provides a correction for the area contacting the lands on impact which corrects for the "negative" curvature of the bore surface (compared to that used as a basis in the Hertz calculations); since the radii of curvature will differ in the two direction of the two major axes, this must be reflected by introducing ℓ_b to scale the radius of curvature in the direction parallel to the tube axis. We thus obtain:

$$t_2 = 2.94 \left[\frac{15}{16} \left(\frac{1 - \sigma_2^2}{q_1} + \frac{1 - \sigma_2^2}{q_2} \right) m \right]^{2/5} \left[\frac{1}{\xi v} \sqrt{\frac{(r - b)}{r b \ell_b}} \right]^{1/5} \quad (94)$$

which together with Equations (89) and (90) provide an expression for the coefficient of restitution.

In the case of the 8" Howitzer XM201 with the M106 HE shell we have

$$\rho_1 = 7.85 \text{ g/cm}^3 = 0.2833 \text{ lbs/in}^3$$

$$\sigma_1 = \sigma_2 = 0.3$$

$$q_1 = q_2 = 3 \times 10^7 \text{ psi}$$

$$\xi = 0.4$$

$$r = 4.0015''$$

$$b = 3.9875''$$

$$\ell_b = 64.0''$$

$$b_1 = 2.252'' \text{ (near the breech of the gun)}$$

and from Figure 4 an average value for ϵ_0 is 3 Joules giving $v = 8.34''/\text{sec}$. These values gives:

$$t_2 = 7.35 \times 10^{-4} \text{ sec} \quad (95)$$

and

$$e = \begin{cases} 0.566, & \kappa = 0.56 \\ 0.642, & \kappa = 0.44 \\ 0.676, & \kappa = 0.39. \end{cases} \quad (96)$$

In the calculations below we have used $e = 0.7$.

VI. APPLICATION TO THE 8" HOWITZER TUBE XM201 MECHANICAL
FAILURE OF APRIL 11, 1974

On April 11, 1974, while firing with temperature conditioned M106 HE the shell broke up in the gun tube and produced moderate to heavy damage to the tube. The test of the Equipment Performance Report is given in Appendix I.

Damage to the tube as described in the Star gage report of 11 April, 1974 (by P. Booth, J. McWilliams, and R. Kane, Appendix I) itemizes:

- a. "Driving and non-driving edge of one land sheared away between 185.00" and 186.75" from (RFT)." This shear is symmetric to the center line of the land (midpoint of damage at 185.88".)
- b. "Heavy to moderate damage to lands encircling bore between 249.75" and 258.50" from (RFT). Damages consist of lands flattened and compressed... From this point forward edges of lands have split away and sprung out from the base of the land for a distance of about 8"...." Again, shearing is in general symmetric about the land center line. Shear planes generally meet at the center line toward breach end of shear and taper off toward land edges toward the muzzle end of the shear (midpoint of damage at 254.12", 68.25" from midpoint of last damage).
- c. "Moderate to light [similar to "b" above] damage to 8 lands between 273.75" and 280.75" (RFT)." (Midpoint of damage at 277.25"; this is 23.12" from midpoint of last damage).
- d. The maximum increase in bore diameter was 20/1000th inch for the lands and 7/1000ths for the grooves.

The shear and flattening damage to the lands indicates a high loading normal to the top surface of the damaged lands. Since the magnitude of the increase in tube diameter was slight, initiation of the HE as a cause of damage is not indicated. Similar (principal) damage appearing in several parts of the tube also argues against HE initiation. The residual TNT after the shot and the fact that the fuze exited the muzzle intact also argue against HE initiation as a cause of the damage. The time-pressure record (see Appendix I) for this shot was, except for small increase late in the strain record, normal. The small spikes in the strain record are consistent with the present interpretation (this is discussed further in Appendix I).

The play in the shell between the bourrelet and lands is estimated to have been 0.014" (all around the shell; i.e., a full swing of the shell would have been 0.028") before impact engraving and about 0.024" to 0.03" after engraving of the bourrelet. These values are obtained from the tube lands diameter in the undamaged regions as given by the Stargage report to be 8.003", the average bourrelet diameter measured on other shells in lot CSK 1-136 yielding an average of 7.988" at normal

temperature and 7.975" at -70°F (the shell temperature at failure). Computer stress-strain calculations for the M106 shell show an increase in bourrelet diameter of +0.0046" at peak pressure and -0.0042" at zero base pressure. At the point of major damage, normal bourrelet deformation would be small (about 0.001").

The tube tested (XM201) extends beyond old tube (in M110 Howitzer). Damage of the type described in paragraph 2b,c above would lie beyond the 210.74" (RFT) position of the muzzle for the M110 Howitzer tube. Characteristic dimensions for shells from the same lot as that which broke up are listed in Table 1.

Using this data let us now determine if the conditions for the development of balloting motion after Equation (80) as given by Equations (81) - (84) were satisfied. As shown by the results in Figure 4, condition (Equation 84) is generally satisfied. The sound velocity in the shell for the calculation of τ_e using Equation (40) is given by (see Raman⁶)

$$c_s = \frac{\pi b_2}{\lambda} \sqrt{q_2/3 \rho_2 (1 - \sigma_2^2)} \quad (97)$$

where the subscripts refer to the appropriate values for the shell. The quantity b_2 is the wall thickness of the shell and λ is wave length of flexural waves in the shell. The wave length of the principal mode will be:

$$\lambda = 4 \sqrt{\pi^2 b^2 + a^2} \quad (98)$$

Using Equations (97) and (98) in Equation (40) gives:

$$\tau_e = 1.64 \times 10^{-3} \text{ sec.} \quad (99)$$

Comparing Equations (95) to (99) we see that condition (82) is satisfied. Further, using that same value of ϵ in Equation (75) we see that

$2c/a\dot{\theta} = 4.72 \times 10^{-3}$ sec so that condition (83) is satisfied. Finally substituting for γ , using handbook values of $\nu = 0.55$ and $\mu = 0.50$ and $n = 20$, we obtain

$$\gamma = 140.6 \quad (100)$$

which, being positive, satisfies the condition of Equation (81).

It should be noted that the coefficients of friction are not constants under the conditions of gun firing. A precise calculation,

Table 1. 8" Shell M106 with Fuze M73 Dummy

Lot No. CSK-1-136 (10P 17-75) with 1 Suppl. Change

Shell No.	Diameters (inches) Front					Total Weight (lbs)	Total Length (inches)	C of G (inches) From Base of Shell	Moments Of Inertia (lbs Ft ²)	
	Bourr.	Above Band	Below Band	Rotating Band	Band Lip				Axial	Transverse
136 v	7.985	7.972	7.973	8.141	8.281	200.48	35.00	12.17	12.7266	101.3459
H	7.985	7.972	7.973	8.141	8.281					
150 v	7.989	7.971	7.973	8.138	8.279	201.14	35.10	12.16	12.7266	101.7727
H	7.988	7.971	7.974	8.139	8.279					
151 v	7.988	7.971	7.973	8.139	8.279	201.28	35.03	12.19	12.7003	101.5592
H	7.988	7.972	7.973	8.139	8.279					

using a computer to follow the details of the balloting should make use of variations in μ and ν as may be obtained from Bowden and Taylor⁸, for example.

Now using Equation (100) in Equation (80), taking ϵ_0 from the computed values given in Figure 4 and allowing for the requirement that t as used in Equation (80) satisfy the constraint:

$$t_s = t + \Delta t_0 \quad (101)$$

where Δt_0 is the time to develop the initial energy ϵ_0 and t_s is the time at which the shell exists the muzzle we can compute the energy ϵ at the end of the muzzle as a function of δ_0 . The result as computed is given in Figure 6. The value of δ_c in Equation (85) is taken as 0.0070, 0.0088, 0.0097 and 0.0106 corresponding to a CG off the geometric axis by 0.040", 0.050", 0.055" and 0.060". The results show the extreme sensitivity of the results to the location of the CG.

From Figure 6, we see that the balloting energy exceeds 10^4 Joules for a CG 0.055" off axis if the initial position of the shell axis lies in a region between $\delta_0 = 0.0011$ and 0.0016 radians as shown in Figure 6. Such an energy corresponds to that required to produce the observed deformation of the gun tube (8 to 10 K Joules) as occurred in the XM201 8" Howitzer mechanical failure. Further, the pressure acting on the lands due to the impact of a shell with 2800J in the balloting mode on the 3.49 in² (projected area) contacting the lands at the bourrelet in a severe impact will subject the lands to a pressure of 150Ksi which is sufficient to cause the observed shear damage to the lands.

If all possible initial values of δ_0 are equally likely, the probability that the shell will lie in this⁰ region is about 0.068 for a CG 0.055" off axis corresponding to a chance of 1 in 15 for the build up in energy by balloting. In addition, δ_c must be off axis as mentioned above. A value of 0.055" off axis for the CG of the shell is not probable but can occur under the allowed tolerance specified for the shell. The rough handling of the shell which led to break up of the charge in the shell also can contribute to the off axis CG. It should be noted that this value of 0.055" is approximate since the coefficient of friction can vary considerably from the values used.

We thus find that the equations obtained in this report allow one to calculate the conditions under which balloting can build to severe levels and produce gun tube damage.

The calculations indicate the following scenario for the XM201 8" Howitzer mechanical failure. Onset of balloting was initiated by an initial high torque due to CG lying off the shell axis. Balloting under the test conditions developed severely enough to cause early engraving of the bourrelet of the shell, leading to increased play at the bourrelet.

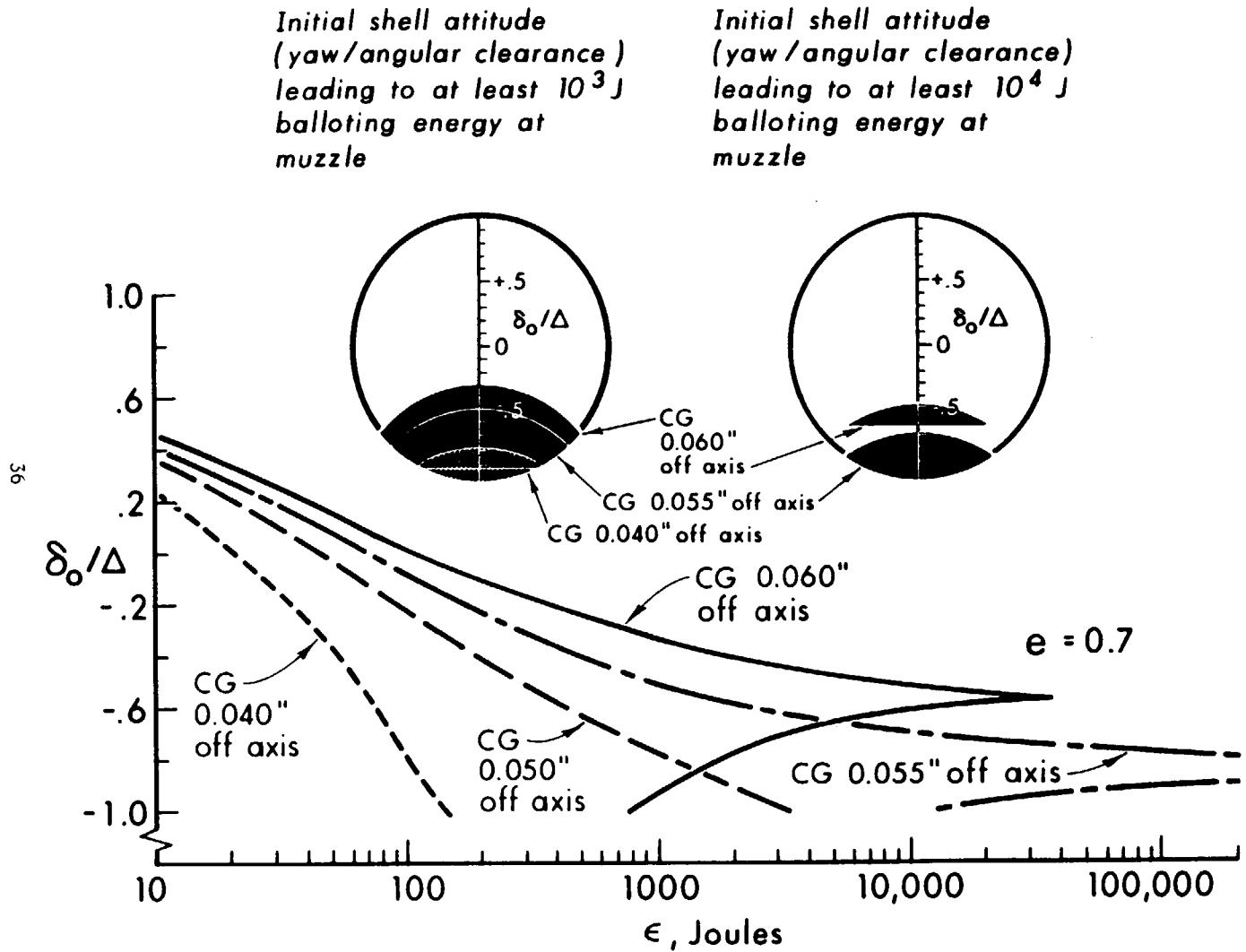


Figure 6. Plot of the energy ϵ in the balloting mode at the muzzle of the gun tube as a function of the initial shell altitude (initial yaw angle divided by the maximum possible yaw) computed from Eqs. (80) and (101) using the results the integration of Eq. (85) shown in Figure 4 and with a coefficient of restitution e of 0.7 and $\gamma = 140.6$ as appropriate for the conditions of the 8" M106 HE shell at -70°F , the XM188 zone 9 charge at -70°F fired in the XM201 Howitzer tube. Several values of position of the shell's center of gravity off axis are used in these calculations. The CG, shell axis and bore axis are all assumed to lie in a single plane. The corresponding solid angles leading to at least 10^3J and 10^4J for all possible initial positions (i.e., CG, shell axis and bore axis not necessarily in a plane) are shown in the inserts. It will be noticed that only a narrow range values of the CG off axis leads to large balloting energies and only if the shell as initially loaded lies in an allowed altitude.

The resulting enhanced balloting caused the shearing of the lands at 185" (RFT) noted in Appendix I and perhaps some shell fracture while momentarily reducing the balloting. Further increase in balloting resulted in the damage between 249.75" and 258.50" (RFT). The major fracturing of the shell would be expected at this point, but not shell breakup. The damage at 277" (RFT) indicates a final buildup of balloting, producing the typical shear failure of the lands and the final breakup of the shell.

As already mentioned, the coefficient of friction can rise significantly as balloting increases pressure between the shell and bore of the gun which can result in binding between the metal surfaces which causes striping of the metal. Such failure of the metal is observed 9" before the major damage and again 9" before the final damage. The appearance of this damage is exactly the same as is shown in Figure 5, plate XXXII of Reference 8. Note that 9" is the distance between the rotating band and the bourrelet.

It is significant that the damage to the lands occurs in the portion of the XM201 tube that has been added to the old 8" Howitzer tube. This alone is not the cause of the failure, however. The large clearance of the shell and asymmetry caused by an off axis CG are additional causes of the growth of violent balloting that produced breakup of the shell and gun tube damage.

A six degree of freedom formulation for the transverse motion of an accelerating shell has been given by Chu and Soechting⁸, and extended in an application to the 8 inch projectile in the XM201, M2A2 gun tube, MK-16 and MCLG Gun by Chu⁹. These papers have the advantage that the effect of shell flexure as a function of shell wall thickness and gun tube flexure are included in the formulation. The formulation does not include the coefficient of restitution nor the very important time delay between bourrelet impact and the reaction force at the rotating band. Excluding this latter effect removes the frictional forces as significant contributors to the development of balloting motion. Although these formulations are quite superior to those of Reno¹ and Thomas², no terms are included that would significantly (i.e., by an order of magnitude) alter their results for the lateral force exerted by the shell on the bore as computed by Gay³ for the case of bore riding. Gay does not find the large forces reported by References 9 and 10. The balloting process involving the buildup of energy in the transverse mode through cumulative, driven impacts by a shell with (excessive) clearance at the bourrelet is not incorporated into the formulations of References 9 and 10. This should not detract from the significant accomplishment of Chu and Soechting's work.

ACKNOWLEDGMENTS

I wish to acknowledge the assistance and encouragement of Dr. Coy Glass who suggested this problem; Mr. Pak Yip who ran computer calculation and to Mr. Ronald Hendrickson and Mr. Robert Huddleston of MTD who furnished much of the data used in the calculations.

REFERENCES

1. F. V. Reno, "The Motion of the Axis of a Spinning Shell Inside the Bore of a Gun," Ballistic Research Laboratories Report No. 320 (AD 491839), Aberdeen Proving Ground, Maryland, February 1943.
2. L. H. Thomas, "The Motion of the Axis of a Spinning Shell Inside the Bore of a Gun," Ballistic Research Laboratories Report No. 544 (AD PB22102), Aberdeen Proving Ground, Maryland, May 1945.
3. H. P. Gay, "Notes on the Yawing Motion of a Projectile in the Bore," Ballistic Research Laboratories Report No. 2259 (AD 908456L), Aberdeen Proving Ground, Maryland, January 1973.
4. H. Goldstein, *Classical Mechanics*, Addison-Wesley Publishing Co., Inc., Cambridge, MA, March 1956.
5. H. Hertz, *J.f. Math. (Crelle)*, Bd. 92 (1881).
6. C. V. Raman, "On Some Applications of Hertz's Theory of Impact," *Phys. Rev.* 15, 277-284 (1920).
7. A. E. H. Love, A Treatise on The Mathematical Theory of Elasticity, Dover Publications, N.Y. 1944.
8. F. P. Bowden and D. Taylor, The Friction and Lubrication of Solids, Clarendon Press, Oxford, G. B., 1950.
9. S. H. Chu and F. K. Soechting, Transverse motion of an accelerating shell, Technical Report 4314, Picatinny Arsenal, Dover, NJ, June, 1972. AD 894572L
10. S. H. Chu, Transverse Motion of 8 inch projectile, XM673, in the XM201, M2A2 Gun Tube, MK-16 and MCLG Gun, Technical Memorandum 2103, Picatinny Arsenal, Dover, NJ, August, 1973.

APPENDIX I

EQUIPMENT PERFORMANCE REPORT FOR 8" HOWITZER TUBE XM201 MECHANICAL FAILURE OF APRIL 15, 1974

The attached report describes the damage to the 8" Howitzer M110E2 as prepared by Mr. Hendrickson of MTD. A photograph (Figure A-1) of the damage to the tube is included. The stargage measurements and inspection data forms for the malfunction as prepared by P. Booth, J. McWilliams and R. Kane is also attached herewith.

Figures A-2 and A-3 give the pressure time records for the mechanical failure. Three tourmaline gages were located at 10", 29.65" and 42.90" (RFT), (i.e., at the spindle, chamber center and forcing cone locations). Figure A-2 shows a computer data reduction giving the difference between the measurements for the gages located at 10" and at 42.90" (RFT). Figure A-3 shows the computer plots for the three gages (channel 1 located at 10" (RFT), channel 2 at 29.65" (RFT)). The kicks in the PT trace are consistent with the interpretation that a pressure pulse propagated into the chamber, reflected off the rear face of the chamber and propagated back up the gun tube. In so doing, the pulse passed gage #1 once and gages #2 and #3 twice. The propagation velocity for the wave is 3000 ft/sec. At this velocity, the time required for a pressure wave to propagate from the position of the shell base at the beginning of the major damage to gage #1 is 5.0 msec. Since from Figure 5 the shell should arrive at the position of major damage at 9.5 msec after the pressure peak and since the pressure peak occurs at 13.0 msec in Figure A-3 (the zero time between Figures 5 and A-3 differs by about 7 msec), a pressure pulse associated with this event should arrive at strain gage #1 at 27.5 msec. The observed time is 27.25 msec. Essentially the same conclusion has already been reached by Ingo May of IBL in his consideration of the PT record of this event.

EQUIPMENT PERFORMANCE REPORT

1. FROM Commander U. S. Army Aberdeen Proving Ground Aberdeen Proving Ground, Maryland 21005		2. OFFICE SYMBOL: STEAP-MT-A	
		3. DATE: 15 Apr 74	
5. TO See Distribution List		4. EPR NO. (K-2)-102	
		6. USATECOM PROJ NO. 2-WE-200-110-004 ROTB E PROJ NO. CONTRACT NO.	
7. TEST TITLE Engineering Test of M110E2, SP, Full-Track, 8-Inch Weapon System			
I. MAJOR ITEM DATA			
8. MODEL Howitzer, SP, 8-Inch, M110E2		9. SERIAL NO.	
10. QUANTITY 1		11. LIFE PERIOD	
12. MFR.		13. USA NO.	
II. PART DATA			
14. NOMENCLATURE / DESCRIPTION Tube, 8-Inch, XM201, Serial No. 12			
15. FSN		16. MFR. PART NO.	
17. DRAWING NO.		18. MFR.	
19. QUANTITY 1		20. NEXT ASSEMBLY	
21. STD. GOVT. GRP.		22. PART TEST LIFE 142 Rounds	
III. INCIDENT DATA			
23. OBSERVED DURING		25. INCIDENT CLASS	
a. OPERATION		X a. DEFICIENCY	
b. MAINTENANCE		b. SHORTCOMING	
c. Firing		c. SUG. IMPROVEMENT	
		d. OTHER	
24. TEST ENVIRONMENT Firing with temperature condi- tioned ammunition		26. ACTION TAKEN	
		a. REPLACED	
		b. REPAIRED	
		c. ADJUSTED	
		d. DISCONNECTED	
		e. REMOVED	
27. DATE AND HOUR OF INCIDENT 11 Apr 74, 1100		X f. NONE Firing Support	
IV. INCIDENT DESCRIPTION			
28. DESCRIBE INCIDENT FULLY			
<p>1. While firing the M110E2 howitzer at 140 mils elevation, the M106 projectile broke up in bore damaging the tube. The projectile had an M557 fuze set superquick and was launched with an XM188 Zone 9 charge. Fragments from the projectile damaged a steel tower velocity cage and coils, instrumentation bombproof, and camera tripod located in front of the muzzle. No personnel injuries resulted.</p> <p>2. Damage to the weapon consisted of moderate to heavy land damage between 245 and 250 inches from the rear face of the tube (See inclosed photograph). Star-gage readings of the groove diameters also indicated a slight bulge in this same region.</p> <p>3. Ammunition involved in the malfunction included the following:</p> <p>a. Projectile, 8-Inch, M106, HE, Lot No. 10P 17-75</p> <p>b. Fuze, PD, M557, Lot No. MA 19-3</p> <p>c. Charge, Propelling, 8-Inch, XM188, Lot No. IND-E-116-74</p>			
DEFICIENCIES AND SHORTCOMINGS ARE SUBJECT TO RECLASSIFICATION			
29. DEFECTIVE MATERIAL SENT TO: Held at APG			
30. NAME, TITLE & DEL EXT. OF PREPARER <i>Ronald Hendricksen</i> RONALD HENDRICKSEN Test Director FA, AA, & Sp Ammo Sec, Arty Ammo Br, Arty Div, MTD, Ext. 2267		31. FOR THE COMMANDER <i>H. B. Anderson</i> H. B. ANDERSON Acting Chief, Artillery Division, Material Testing Directorate	

Equipment Performance Report (K-2)-102

Title: Engineering Test of M110E2, SP, Full-Track, 8-Inch Weapon System
TECOM Project No. 2-WE-200-110-004

Each of the ammunition components had been subjected to sequential rough handling tests at -70°F prior to firing. The specific rough handling conditions for each component were as follows:

(1) The projectile had been dropped 7-feet unpackaged to impact a steel plate base first with the axis 45° from the vertical. Following this, the projectile was subjected to a bounce test with the projectile in its normal vertical orientation.

(2) The fuze was subjected to successive 7-foot drops in six different orientations while in its normal packaging. Following this, the packaged fuze was bounce tested with the fuze horizontal. Finally, the fuze was affixed to a 105-mm M1 shell and dropped 5 feet so as to strike nose down with the shell 45° from the vertical.

(3) The packaged propelling charge was dropped 7 feet so as to strike the steel plate with the base end of the charge down and the charge 45° from the vertical. Then the charge was bounce tested with the charge vertical, base charge end down. Finally, the unpackaged charge was dropped horizontally and base down from a height of 5 feet.

Following each phase of the rough handling sequence, each component was visually inspected to establish if the items were safe to continue testing. At the end of the sequence, all components were visually inspected. In addition, the projectiles and fuzes were x-rayed to examine for internal damage. X rays of the projectile involved in the malfunction showed cracks in the TNT filler between the forward bourrelet and the nose of the shell. The fuze showed slight visual damage to the nose of the fuze but no internal damage. The propelling charge suffered a seam rip after two of the planned five drops. This rip was mended before firing, but no further drops were conducted.

4. At the time of firing, the ambient air temperature was 53°F. All ammunition components were temperature conditioned to -70°F. The malfunction occurred on the eighth round of the day and 11th test round of the safety test. Comparison data for the malfunctioned round and the previous test rounds combined are provided in the following table.

Equipment Performance Report (K-2)-102

Title: Engineering Test of M110E2, SP, Full-Tracked, 8-Inch Weapon System
 TECOM Project No. 2-WE-200-110-004

Comparison Data for M110E2 Safety Test Firings -
 Malfunctioning Versus Nonmalfunctioning Rounds

Type of Rd	No. of Rds	Preconditioned	Firing Temperature, °F	Seating, In	Avg Peak Pressure, KSI	Avg Vel fps	Avg Recoil, In	Avg RC, M
Malfunc- tion	1	RH	-70	44 1/2	36.1	NA	49 1/2	NA
Test	10	RH	-70	44 3/8	36.7	2457	49 7/8	9532

There were two small kicks in the PT trace 17 milliseconds after the peak pressure was reached, but otherwise the trace was normal and similar to previous test rounds.

5. Investigation of the incident is continuing.

1 Incl
 Photograph

DISTRIBUTION LIST

Equipment Performance Report
Engineering Test of M110E2, SP, Full-TrackeD, 8-Inch Weapon System
TECOM Project No. 2-WE-200-110-004

<u>Addressee</u>	<u>No. of Copies</u>
Commander U. S. Army Test and Evaluation Command ATTN: AMSTE-FA Aberdeen Proving Ground, Maryland 21005	1
Commander U. S. Army Materiel Command ATTN: AMCRD-WC 5001 Eisenhower Avenue Alexandria, Virginia 22304	1
Commander U. S. Army Armament Command ATTN: AMSAR-RDG Rock Island Arsenal Rock Island, Illinois 61201	1
Commander U. S. Army Systems Analysis Agency ATTN: AMXSY-RE Aberdeen Proving Ground, Maryland 21005	1
Commander U. S. Army Logistic Evaluation Agency ATTN: LEA-IL New Cumberland Army Depot New Cumberland, Pennsylvania 17070	1
Commander U. S. Army Maintenance Management Center ATTN: AMXMD-IDV Lexington, Kentucky 40507	1
Commandant U. S. Army Field Artillery School ATTN: Field Artillery Agency Fort Sill, Oklahoma 73503	1

Equipment Performance Report
 Engineering Test of M110E2, SP, Full-TrackeD, 8-Inch Weapon System
 TECOM Project No. 2-WE-200-110-004

<u>Addressee</u>	<u>No. of Copies</u>
Commander Picatinny Arsenal ATTN: SARPA-AD-E	1
SARPA-AD-F	1
SARPA-AD-M	1
SARPA-QA-A	1
Dover, New Jersey 07801	
 Commander Watervliet Arsenal	1
Watervliet, New York 12189	
 President U. S. Army Field Artillery Board	1
Fort Sill, Oklahoma 73503	
 Commander U. S. Army Training and Doctrine Command	
ATTN: ATCD-C	1
Fort Monroe, Virginia 23651	
 Commander U. S. Army Combined Arms Combat Development Activity	
ATTN: ATCACS-P	1
Fort Leavenworth, Kansas 66027	
 Commandant U. S. Army Ordnance Center and School	
ATTN: ATSL-LTD	1
Aberdeen Proving Ground, Maryland 21005	
 Commander Rock Island Arsenal	
ATTN: SARRI-LA	1
Rock Island, Illinois 61201	
 Commander U. S. Army Aberdeen Proving Ground	
ATTN: STEAP-MT-A	1
Aberdeen Proving Ground, Maryland 21005	

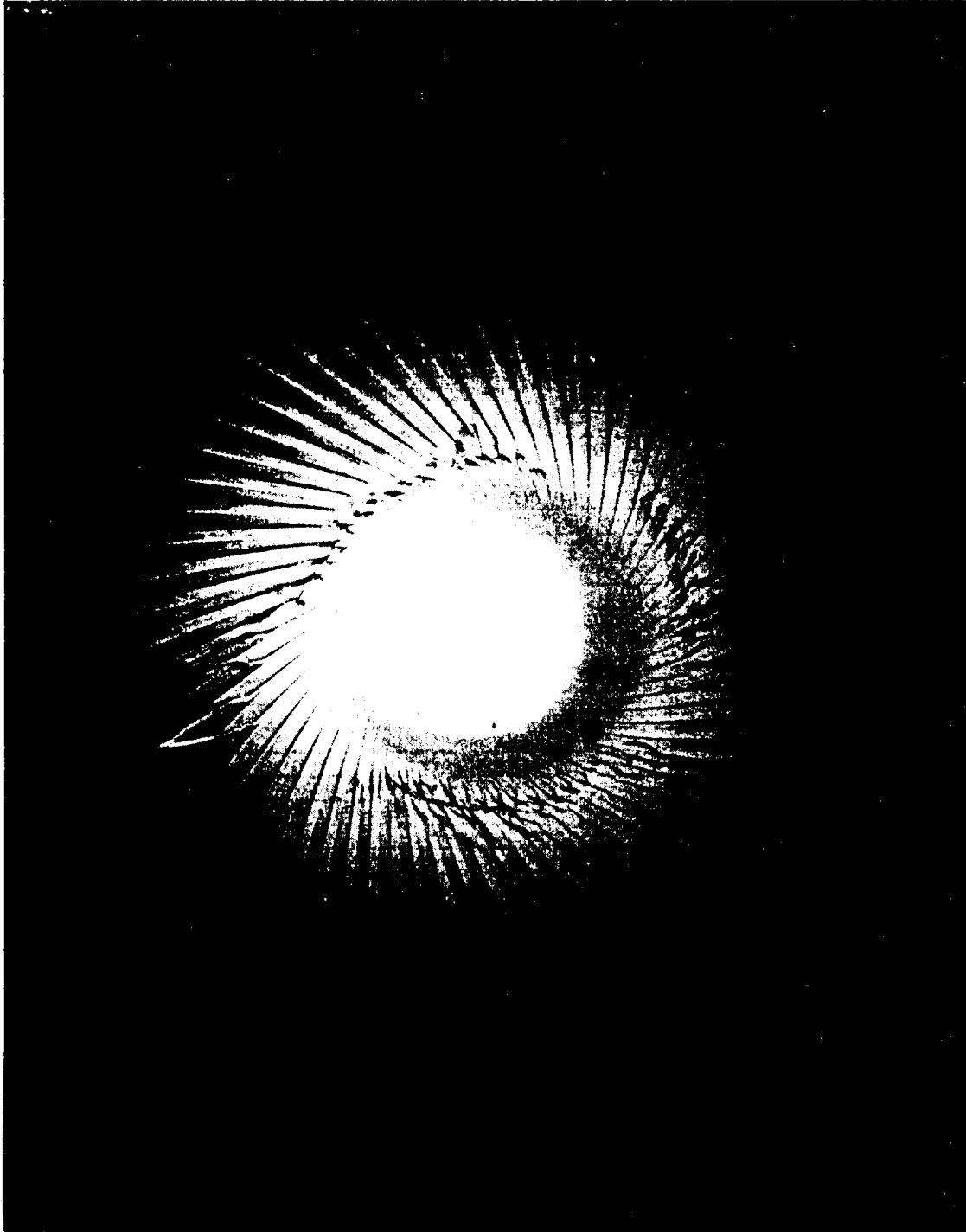


Figure A-1. Photograph of damage to the 8" XM201 Howitzer Tube
looking from the Muzzle end.

MULTIPLE STARGAGE MEASUREMENT & INSPECTION DATA FORM

8.00" HOWITZER TUBE XM201 MOD.		Main bore = 46.32" to 315.86"					
DISTANCE (Inches)	From -		Zero Ref., indicated in 1/1000 of an inch				
	REAR FACE OF BREECH	MUZZLE FACE	REAR FACE OF TUBE	8.000" LANS Basic Dia.		8.140" Groove Dia.	
			Vert.	Hor.	Vert.	Hor.	
322.35	.61	315.25	+ .006	+ .005	.000	.000	
322.10	.86	315.00	4	3	0	0	
317.10	5.86	310.00	2	2	0	0	
312.10	10.86	305.00	2	2	0	0	
307.10	15.86	300.00	2	2	0	0	
302.10	20.86	295.00	2	2	0	0	
297.10	25.86	290.00	3	3	0	+ .001	
292.10	30.86	285.00	3	4	+ .001	1	
287.10	35.86	280.00	5	5	1	1	
282.10	40.86	275.00	9	7	2	1	
277.10	45.86	270.00	10	7	4	1	
272.10	50.86	265.00	10	7	4	1	
267.10	55.86	260.00	9	7	5	1	
262.10	60.86	255.00	16	13	7	1	
257.10	65.86	250.00	20	9	3	.000	
252.10	70.86	245.00	2	5	.000	0	
247.10	75.86	240.00	2	5	0	0	
242.10	80.86	235.00	2	4	0	0	
237.10	85.86	230.00	3	3	0	0	
232.10	90.86	225.00	3	3	0	0	
227.10	95.86	220.00	3	3	0	0	
222.10	100.86	215.00	3	3	0	0	
217.10	105.86	210.00	3	3	0	0	
212.10	110.86	205.00	3	3	0	0	
207.10	115.86	200.00	3	3	0	0	
202.10	120.86	195.00	3	4	0	0	
197.10	125.86	190.00	3	4	0	0	
192.10	130.86	185.00	3	4	0	0	
187.10	135.86	180.00	3	4	0	0	
182.10	140.86	175.00	3	4	0	0	
177.10	145.86	170.00	3	4	0	0	
172.10	150.86	165.00	3	4	0	0	
167.10	155.86	160.00	3	4	- .001	0	
162.10	160.86	155.00	3	4	1	0	
157.10	165.86	150.00	3	3	1	0	
152.10	170.86	145.00	3	3	1	0	
147.10	175.86	140.00	2	3	1	- .001	
142.10	180.86	135.00	2	3	2	1	
137.10	185.86	130.00	2	4	2	1	
132.10	190.86	125.00	3	4	2	1	
127.10	195.86	120.00	3	4	2	1	
122.10	200.86	115.00	3	5	2	1	
117.10	205.86	110.00	4	5	2	1	
112.10	210.86	105.00	4	5	2	1	
107.10	215.86	100.00	4	5	2	1	
102.10	220.86	95.00	4	5	2	1	
97.10	225.86	90.00	3	4	2	2	
92.10	230.86	85.00	2	3	2	2	
87.10	235.86	80.00	1	2	2	2	
82.10	240.86	75.00	1	1	2	2	
77.25	245.71	70.00	1	1	1	2	
72.10	250.86	65.00	1	1	1	2	
69.25	253.71	62.15	2	1	1	2	
67.10	255.86	60.00	3	2	.000	2	
61.25	261.71	54.15	.003	+ .002	- .000	2	
259.00	(MAX. READING)		+ .026	+ .017	+ .007	+ .001	

8.00" Howitzer Tube XM201 MOD.

Chamber 2.51" to 46.15

DISTANCE (Inches) FROM				GAUGE MEASUREMENTS INDICATED IN 1/1000 OF AN INCH						
REAR FACE OF BREECH	MUZZLE FACE	REAR FACE OF TUBE	BASIC DIAMETER	HEAD			TAIL			
				GAUGE READING	ACTUAL DIAMETER	DIFFERENCE	GAUGE READING	ACTUAL DIAMETER	DIFFERENCE	
50.10	272.86	43.00	8.300	-.005	8.295	-.005	-.005	8.295	-.005	5
49.10	273.86	42.00	8.305	+ .002	8.302	-.003	+ .002	8.302	-.003	3
47.10	275.86	40.00	8.311	11	311	3	10	310	4	4
45.10	277.86	38.00	8.323	19	319	4	19	319	4	4
43.10	279.86	36.00	8.332	28	328	4	28	328	4	4
41.10	281.86	34.00	8.341	37	337	4	37	337	4	4
39.10	283.86	32.00	8.350	46	346	4	46	346	4	4
37.10	285.86	30.00	8.359	55	355	4	55	355	4	4
35.10	287.86	28.00	8.368	64	364	4	64	364	4	4
33.10	289.86	26.00	8.377	73	375	2	75	375	2	2
31.10	291.86	24.00	8.386	84	384	2	84	384	2	2
29.10	293.86	22.00	8.395	94	394	1	94	394	1	1
27.10	295.86	20.00	8.404	104	404	.000	104	404	.000	
25.10	297.86	18.00	8.413	111	411	-.002	111	411	-.002	
23.10	299.86	16.00	8.422	119	419	3	119	419		
21.10	301.86	14.00	8.431	128	428	3	129	429	2	2
19.10	303.86	12.00	8.440	138	438	2	138	438	2	2
17.10	305.86	10.00	8.449	147	447	2	148	448	1	1
15.10	307.86	8.00	8.458	156	456	2	158	458	.001	
13.10	309.86	6.00	8.467	165	465	2	167	467	0	
11.10	311.86	4.00	8.476	175	475	1	176	476	0	
9.10	313.86	2.00	8.485	185	485	.000	186	486	+ .001	
8.70	314.26	1.60	8.487	+ .188	8.488	+ 1.001	+ .184	8.489	+ .002	

0.300

8" TUBE, #14 XM201 MOD. FOR: MR HENRICKSON W.O. 305-95401-02

SPECIAL MEASUREMENTS

	BASIC	ACTUAL		BASIC	ACTUAL
TOTAL LENGTH OF GUN	322.96"	—	ROTATION OF TUBE AT BREECH	—	—
TOTAL LENGTH OF TUBE	315.86"	315.85"	MOVEMENT OF TUBE AT BREECH	—	—
DEPTH OF BREECH RECESS	7.10"	—	NUMBER OF LANDS AND GROOVES	64	64

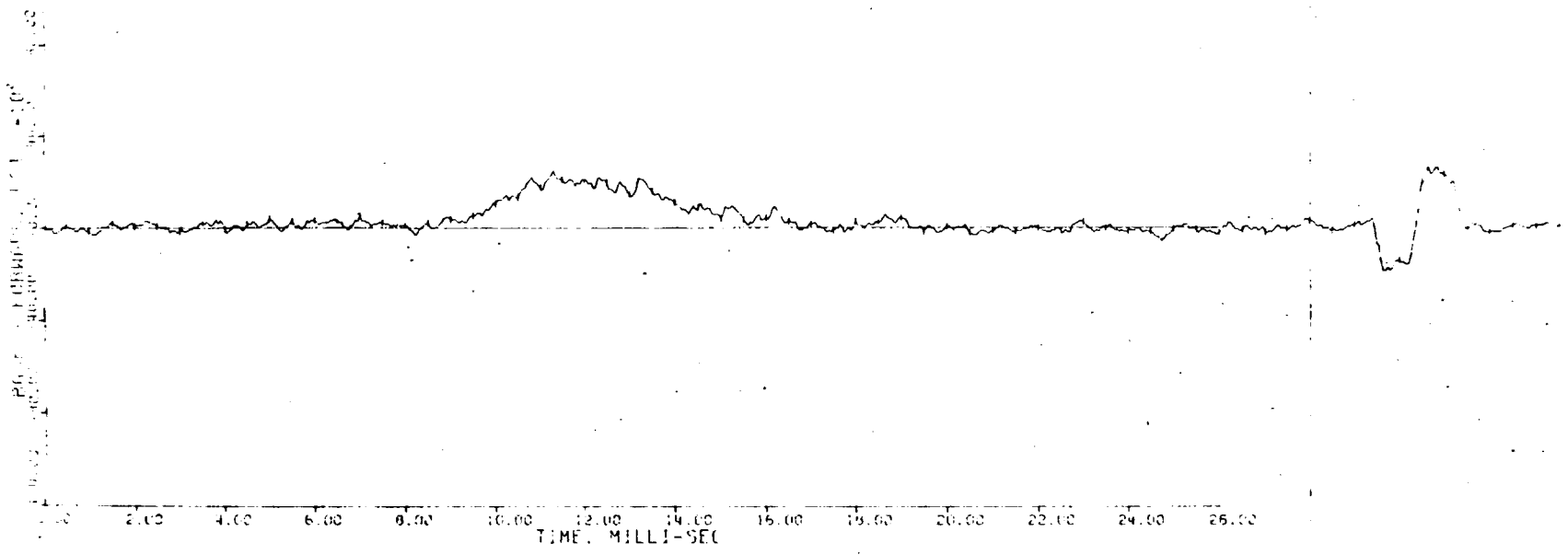
Inspection Remarks: Areas from 0.00 to 1.50", 43.10" to 46.15" and from 315.25" to 315.86" were not measured.

STAMPED PREV. APG.	STARGAUGED AND INSPECTED BY BOOTH	REVIEWED BY
ROOMMAN M ^W WILLIAMS	TIME	COMPILATOR
RECORDER KANE	PLACE 525	

MULTIPLE STARGAGE MEASUREMENT & INSPECTION DATA FORM

8.00" Howitzer Tube XM201 MOD.	
CASTING NUMBER	Main Bore - 46.12" to 315.86"
	Gage Meas. indicated in 1/1000 of an inch
MANUFACTURER	LANDS
	8.000" Basic Dia. 8.110" Basic Dia.
MODEL	Vert. Hor. Vert. Hor.
	8.000" Basic Dia. 8.110" Basic Dia.
NUMBER	Vert. Hor.
	8.004" 8.003"
FIRING STATUS (Check One)	Estimated Remaining Accuracy Life
	8
DATE OF GAUGING	SPECIAL MEASUREMENTS
	Basic Actual
8.00" HOWITZER	Opening between breech bushing and rear face of tube
	Top Bottom Right Left
8.00" HOWITZER	Rotation of breech bushing at R.F.T.
	Trammel Distance Est. blished
DATE OF GAUGING	B.F. Rds.
	2.000 1.987
8.00" HOWITZER	2.005 1.954
	2.006 2.029
8.00" HOWITZER	Bore scope Remarks: (Chrome Plated Chamber and Bore)
	Several light longitudinal scratches with light powder fouling, carbon and other deposits thru-out chamber. Light heat checking beginning in centering cylinder and becoming moderate at origin of rifling and extending forward to 60.00" in the grooves and to 140" on lands from rear face of tube (RFT). Chrome lightly chipped on edges of lands encircling commencement of rifling and vicinity. Light powder foulings, carbon and other deposits thru-out bore. Driving and non-driving edge of one land sheared away between 185.00" and 186.75" from (RFT) at 1:00 o'clock. Heavy to moderate damage to lands encircling bore between 249.75" and 258.50" from (RFT). Damages consist of lands flattened and compressed with highly polished brass deposits at 249.75" from (RFT). From this point forward edges of lands have split away and sprung out from the base of the land for a distance of approximately 8.00". Lands are still intact at the flattened area at 259.75" from (RFT). Four lands at 2:00 o'clock, 3 lands at 10:00 o'clock and 5 lands at 8:00 o'clock thru-out this area have not been damaged. Moderate to light similar damage to 8 lands between 273.75" and 280.75" from (RFT) at 2:00 o'clock.
8.00" HOWITZER	Due to damages in bore tube is "HAZARDOUS" in accordance with MTD 750-1, Sec 2, Par. b.
	A series of photos were taken thru-out damaged areas.
8.00" HOWITZER	Gaged By: P. Booth
	J. McWilliams
8.00" HOWITZER	R. Kane

RD NO. 11 91 HOW. DATE FIREP. 11 APR. 1974



49

RD NO. 11 91 HOW. DATE FIREP. 11 APR. 1974

- CHANNEL 1
- △ CHANNEL 2
- + CHANNEL 3
- x CHANNEL 4
- ◇ CHANNEL 5
- CHANNEL 6



Figure A-2. Plot of the pressure difference between strain gage #1 at the spindle and strain gage #3 at the forcing cone as a function of time.

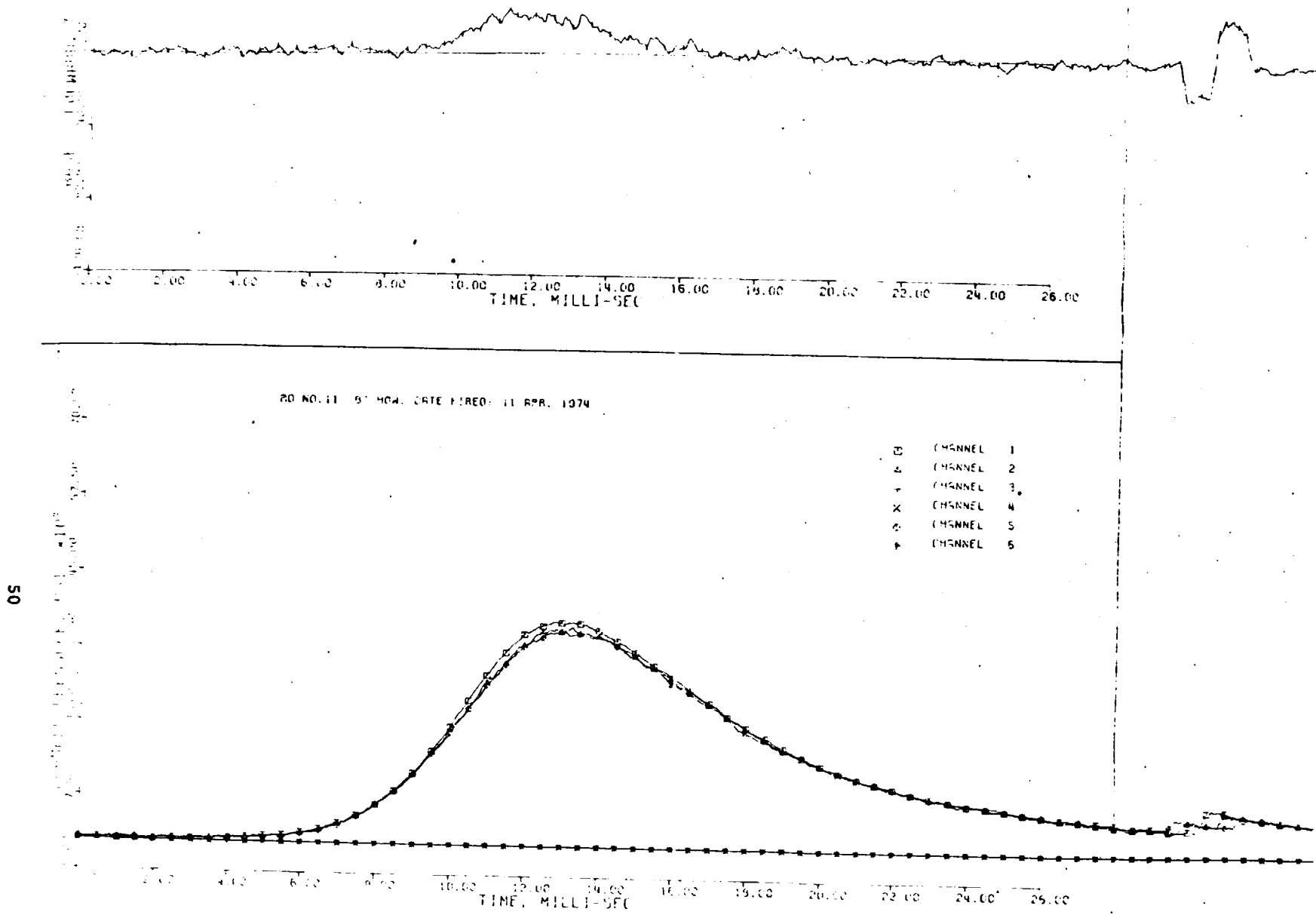


Figure A-3. Plot of the pressure vs. time for three tourmaline strain gages located at the spindle (#1, 10" RFT), middle of chamber (#2, 29.65" RFT) and at the forcing cone (#3, 42.90" RFT).

LIST OF SYMBOLS

a	distance between the center of the bourrelet and rotating band, also, radius of gun tube wall area deflected by shell impact at end of impact ($t = t_2$)	m
b	radius of shell at bourrelet	m
b'	radius of shell at rotating band	m
b_1	half thickness of gun tube wall	m
c	clearance between bourrelet and bore of gun for zero yaw	m
c_s	velocity of sound in shell	m/sec
e	coefficient of restitution	dimensionless
k_a	radius of gyration about shell axis	m
ℓ	distance from CG to the point on shell's axis at center of the rotating band	m
ℓ_b	bourrelet radius of curvature (in cross-section) at point of contact with lands of gun tube	m
m	mass of shell	Kg
m_1, m_2	mass of balls	kg
n	twist of the rifling	(calibers/turn)
P_b	base pressure	newtons/m ²
P_c	chamber pressure	newtons/m ²
q_1, q_2	Young's modulus (gun tube, shell, respectively)	newtons/m ²
q_i, q_1, q_2, q_3	generalized Lagrangian coordinates	(Q_i x q_i have dimensions of energy)
r	radius of gun tube bore	m
r_1, r_2	radius of balls	m
s	distance traveled by shell along z coordinate	m

LIST OF SYMBOLS

t	time	sec
t_s	time from onset of shell motion to shell exit	sec
t_1	time from first contact on impact between bourellet and gun bore to maximum yaw δ_{max}	sec
t_2	time from first contact on impact between bourellet and gun bore to end of impact contact	sec
v	velocity of bourellet at impact with bore	m/sec
x	x-component of rectilinear coordinates fixed with reference to the gun tube; z-component co-linear with gun tube axis	m
x_s	x-component of rectilinear coordinates fixed with reference to the shell; z-component co- linear with shell axis	m
y	y-component of rectilinear coordinates fixed with reference to the gun tube; z-component co-linear with gun tube axis	m
y_s	y-component of rectilinear coordinates fixed with reference to the shell; z-component co-linear with shell axis	m
z	z-component of rectilinear coordinates; co-linear with gun tube axis	m
z_s	z-component of rectilinear coordinates; co-linear with shell axis	m
A	axial moment of inertia	kg m^2
B	transverse moment of inertia	kg m^2
C	the point on the shell's axis at the center of the rotating band	-
C_1	constant of integration	(dimensionless)
C_2	constant of integration	kg m^2
E_s	translational kinetic energy of shell	Joules

LIST OF SYMBOLS

E_{ψ}	spin kinetic energy of shell	Joules
I	moment of inertia about the point on shell's axis at center of the rotating band	kg m^2
I'	constant (see Eq. 27)	(dimensionless)
K_c, K_r	force constant (Hooke's law)	Newtons
L	Lagrangian	Joules
L_e	gun tube length (from forcing cone to muzzle)	m
Q_i	components of the generalized Lagrangian force	($Q_i x_{q_i}$ have dimensions of energy)
Q_1, Q_2, Q_3	components of the generalized Lagrangian force	($Q_i x_{q_i}$ have dimensions of energy)
S	angular acceleration in yaw per $\sin \delta$ (see Eq. 29)	radians/sec ²
T	rotational kinetic energy, also, torque acting on the rotating band due to the <u>rifling</u> (excluding impact and reactions force torques) of the gun tube	Joules Newton-m
\bar{T}_y	time averaged torque for y-components due to impacts	Newton-m
\bar{T}_z	time averaged torque for z-components due to impacts	Newton-m
T'	total torque on shell acting in z-direction ($T' = Q_3$)	Newton-m
V	potential energy of the shell in a coordinate system moving with the shell (accelerating coordinate system)	Joules
X	x-component of impact force acting on bourrelet	Newtons
X'	x-component of impact reaction force acting on rotating band	Newtons
X_1^*	spin up forces of lands against rotating band	Newtons
Y	y-component of impact force action on bourrelet	Newtons

LIST OF SYMBOLS

Y'	y-component of impact reaction force acting on rotating band	newtons
Z	z-component of impact force acting on bourrelet	newtons
Z'	z-component of impact reaction force acting on rotating band	newtons
α	shell spin rate as given by Thomas	radius/sec
δ	yaw angle, inclination of the shell axis from gun tube bore axis	(radians)
δ_c	angle between the shell axis and a line passing through the point C and the CG of the shell	(radians)
δ_o	initial yaw angle of shell as loaded in gun chamber	(radians)
δ_{max}	maximum yaw of shell during impact between bourrelet and gun bore	(radians)
$\dot{\delta}_o$	angular velocity at $\delta = 0$ (zero yaw)	radians/sec
γ	constant (see Eq. 77)	(dimensionless)
ϵ	kinetic energy in the yawing (δ -component only) motion of the shell	Joules
ϵ_o	initial (first impact between bourrelet and gun bore) kinetic energy in the yawing (δ -component only) motion of the shell	Joules
θ	total angle swept out by the shell in the δ direction irrespective of sign	(radians)
κ	Raman's coefficient	(dimensionless)
λ	wave length of flexural waves in shell	m
μ	coefficient of friction between bourrelet and gun tube	(dimensionless)
ν	coefficient of friction between rotating band and gun tube	(dimensionless)
ξ	ratio of lands area to total bore area in gun tube	(dimensionless)

LIST OF SYMBOLS

ρ_1, ρ_2	density (gun tube, shell, respectively)	Kg/m^3
σ_1, σ_2	poisson's ratio (gun tube, shell, respectively)	(dimensionless)
τ_e	time lag between impact on bourrelet and reaction force at rotating band	sec
ϕ	azimuth of the shell about the gun tube bore axis	(radians)
ψ	rotation angle of the shell about its own axis	(radians)
$\omega_x, \omega_y, \omega_z$	components of angular velocity about axes, x, y, z	sec^{-1}
Δt	time between impacts of bourrelet	sec
Δt_o	time from onset of shell motion to first bourrelet impact	sec
$\Delta\phi$	angle of precession during bourrelet impact	sec
Ω	shell spin rate about shell axis	radians/sec
Ω'	constant (see Eq. 28)	radians/sec

DISTRIBUTION LIST

<u>No. of Copies</u>	<u>Organization</u>	<u>No. of Copies</u>	<u>Organization</u>
2	Commander Defense Documentation Center ATTN: DDC-TCA Cameron Station Alexandria, Virginia 22314	1	Commander U.S. Army Electronics Command ATTN: AMSEL-RD Fort Monmouth, New Jersey 07703
1	Director Defense Advanced Research Projects Agency 1400 Wilson Boulevard Arlington, Virginia 22209	1	Commander U.S. Army Missile Command ATTN: AMSMI-R Redstone Arsenal, Alabama 35809
1	Director of Defense Research and Engineering (OSD) Washington, DC 20315	1	Commander U.S. Army Tank Automotive Command ATTN: AMSTA-RHFL Warren, Michigan 48090
1	Commander U.S. Army Materiel Command ATTN: AMCDL 5001 Eisenhower Avenue Alexandria, Virginia 22333	2	Commander U.S. Army Mobility Equipment Research & Development Center ATTN: Tech Docu Cen, Bldg. 315 AMSME-RZT Fort Belvoir, Virginia 22060
1	Commander U.S. Army Materiel Command ATTN: AMCRD, BG H. A. Griffith 5001 Eisenhower Avenue Alexandria, Virginia 22333	1	Commander U.S. Army Armament Command Rock Island, Illinois 61202
1	Commander U.S. Army Materiel Command ATTN: AMCRD-T 5001 Eisenhower Avenue Alexandria, Virginia 22333	4	Commander U.S. Army Frankford Arsenal ATTN: SARFA-MT-211 Abe Korr B. W. Bushey Library SARFA-MDS-B, Charles Dickey Philadelphia, Pennsylvania 19137
1	Commander U.S. Army Aviation Systems Command ATTN: AMSAV-E 12th & Spruce Streets St. Louis, Missouri 63166	5	Commander U.S. Army Picatinny Arsenal ATTN: SARPA-AD-F-D, Mr. Fred E. Saxe Dover, New Jersey 07801
1	Director U.S. Army Air Mobility Research and Development Laboratory Ames Research Center Moffett Field, California 94035		

DISTRIBUTION LIST

<u>No. of Copies</u>	<u>Organization</u>	<u>No. of Copies</u>	<u>Organization</u>
4	Commander U.S. Army Picatinny Arsenal ATTN: SARPA-VAG SARPA-VA SARPA-DE Dover, New Jersey 07801	7	Commander U.S. Naval Ordnance Systems Command ATTN: ORD-04; ORD-04M; ORD-044; ORD-553; ORD-5524; ORD-03; ORD-0332 Washington, DC 20360
2	Commander U.S. Army Watervliet Arsenal ATTN: SARWV-RD, Dr.R.E.Weigle T. E. Davidson Watervliet, New York 12189	1	Chief of Naval Operations Department of the Navy Washington, DC 20350
4	Commander U.S. Army Watervliet Arsenal ATTN: SARWV-RDD, Paul Rummel (2 cys) SARWV-RDD-SP, John Busuttel SARWV-RDD-ATW, Ray Betner Watervliet, New York 12189	1	Chief of Naval Material Department of the Navy Washington, DC 20360
1	Commander U.S. Army Watervliet Arsenal Bennet Research Laboratories ATTN: Richard Hasenbein Watervliet, New York 12189	1	Director of Naval Laboratories Department of the Navy Washington, DC 20360
2	Commander U.S. Army Harry Diamond Laboratories ATTN: AMXDO-TI AMXDO-EDF, M. Ressler Washington, DC 20438	1	Office of Naval Research 800 North Quincy Street ATTN: Dr. W. G. Rauch Arlington, Virginia 22304
1	Commander U.S. Army Materials and Mechanics Research Center Watertown, Massachusetts 02172	1	Superintendent U.S. Naval Academy Annapolis, Maryland 21402
1	HQDA (DAMA-AR, MAJ R.A.Burns) Arlington, Virginia 22209	1	Director Naval Ammunition Production Engineering Center Naval Ammunition Depot ATTN: Code 04MB Crane, Indiana 47522
		1	Commander U.S. Naval Ships Parts Control Center Mechanicsburg, Pennsylvania 17055

DISTRIBUTION LIST

<u>No. of Copies</u>	<u>Organization</u>	<u>No. of Copies</u>	<u>Organization</u>
1	Commander U.S. Naval Weapons Center ATTN: J. Pearson China Lake, California 93555	2	Commander U.S. Naval Weapons Station ATTN: Code 64A, NEDED St. Juliens Annex Yorktown, Virginia 23491
8	Commander U.S. Naval Ordnance Laboratory ATTN: Code 702 Code 231 Code 412 S. Jacobs, D. Price J. Goeller, W. Messick H. Sternberg Silver Spring, Maryland 20910	1	Headquarters U.S. Marine Corps ATTN: Code A04E LTC Mazzaca Washington, DC 20380
2	Commander U.S. Naval Research Laboratory ATTN: W. Pellini Code 7785, Walt Atkins Washington, DC 20375	1	AFATL (DL, Mr. Dale Davis) Eglin AFB Florida 32542
2	Commander U.S. Naval Weapons Laboratory ATTN: EPA, John Foltz GW, Mr. L.M. Williams Dahlgren, Virginia 22448	1	AFAL Eglin AFB Florida 32542
2	Commander U.S. Naval Ordnance Station ATTN: SS73D, Mr. W. Burnett ES43A Indianhead, Maryland 20640	1	Director Lawrence Radiation Laboratory ATTN: M. Wilkins P. O. Box 1663 Livermore, California 94550
1	Commander U.S. Naval Ordnance Station Louisville, Kentucky 40214	1	Sandia Laboratories ATTN: O. E. Jones Albuquerque, New Mexico 87115
1	Commander U.S. Naval Weapons Station ATTN: Code QEL Concord, California 94520		<u>Aberdeen Proving Ground</u> Marine Corps Ln Ofc Dir, USAMSAA Dir, USAMTD ATTN: H. A. Bechtol R. Hendrickson R. L. Huddleston



DEPARTMENT OF THE ARMY
U. S. ARMY ARMAMENT RESEARCH AND DEVELOPMENT COMMAND
U. S. ARMY BALLISTIC RESEARCH LABORATORY
ABERDEEN PROVING GROUND, MARYLAND 21005

DRDAR-TSB

8 March 1978

SUBJECT: Change of Distribution Statement

Commander
Defense Documentation Center
ATTN: DDC-TCA
Cameron Station
Alexandria, VA 22314

A review of the reports listed below has been completed and it has been determined that the distribution limitation can be removed and the Statement "A" be applied:

<u>REPORT</u>	<u>TITLE</u>	<u>DATE</u>	<u>AD NO</u>
BRL Report No. 1406	BRL Survey Of The Army Caseless Ammunition Program.	Jun 68	844887L
BRL Report No. 1756	The Effect Of Muzzle Jet Asymmetry On Projectile Motion.	Jan 75	B002159L
BRL Report No. 1758	Wind Tunnel Magnus Tests Of Cylindrical And Boattail Army-Navy Spinner Projectiles With Smooth Surface And 20MM Equivalent Engraving (Rifling Grooves).	Feb 75	B002628L
BRL Report No. 1793	The Influence Of Muzzle Gasdynamics Upon The Trajectory Of Fin-Stabilized Projectiles.	Jun 75	B005379L
BRL Report No. 1899	Plane Shock - Thermal Layer Interaction.	Jul 76	B013138L
BRL Report No. 1900	The Effect Of Wind On Flat-Fire Trajectories.	Aug 76	B012872L
BRL Report No. 1945	Muzzle Blast Amplification.	Nov 76	B015779L

PROPERTY OF U.S. ARMY
STEINBO BRANCH
BRL ABERDEEN, MD. 21005

DRDAR-TSB
SUBJECT: Change of Distribution Statement

8 March 1978

<u>REPORT</u>	<u>TITLE</u>	<u>DATE</u>	<u>AD NO</u>
BRL Memorandum Report No. 1864	SPIW Modes Of Fire.	Feb 68	388522
BRL Memorandum Report No. 1919	Accuracy Of Rifle Fire: SPIW, M16A1, M14.	Mar 68	390136
BRL Memorandum Report No. 1953	A Comparative Evaluation Of The 7.62MM And 5.56MM, G-3 Assault Rifles.	Jan 69	849576
BRL Memorandum Report No. 2211	Optimum Projectile Shape For Improving Ammunition.	Aug 72	906481L
BRL Memorandum Report No. 2215	A Computer Program To Calculate The Physical Properties Of A System Of Coaxial Bodies Of Revolution.	Aug 72	904378L
BRL Memorandum Report No. 2225	Determination Of Muzzle Velocity Changes Due To Nonstandard Propellant Temperature Using An Interior Ballistic Computer Simulation.	Sep 72	905714L
BRL Memorandum Report No. 2276	Muzzle Devices, A State-Of-The-Art Survey. Volume I: Hardware Study.	Feb 73	909325L
BRL Memorandum Report No. 2281	On The Misuse Of Field Artillery Firing Tables.	Mar 73	909704L
BRL Memorandum Report No. 2337	Verification Of Ground Test Data By Instrumented Flight Test Of An Artillery Shell.	Oct 73	915842L
BRL Memorandum Report No. 2338	An Investigation Into The Flight Characteristics Of Rotating Discs.	Oct 73	914557L
BRL Memorandum Report No. 2381	Boundary-Layer Studies On Spinning Bodies Of Revolution.	May 74	920069L
BRL Memorandum Report No. 2396	Long Range Dynamics Flight Experi- ments With The 155MM Projectile, M483.	Jul 74	922181L

DRDAR-TSB
SUBJECT: Change of Distribution Statement

8 March 1978

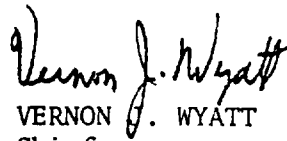
<u>REPORT</u>	<u>TITLE</u>	<u>DATE</u>	<u>AD NO</u>
BRL Memorandum Report No. 2411	Yawing And Balloting Motion Of A Projectile In The Bore Of A Gun With Application To Gun Tube Damage.	Sep 74	923913L
BRL Memorandum Report No. 2456	Effects Of Base Bleed And Super- sonic Nozzle Injection On Base Pressure.	Mar 75	B003442L
BRL Memorandum Report No. 2496	Experiments On Wake Optical Properties.	Jul 75	B005619L
BRL Memorandum Report No. 2501	Preliminary Surveys Of The Three Dimensional Boundary Layer On A Yawed, Spinning Body Of Revolution.	Jul 75	B005829L
BRL Memorandum Report No. 2536	The Effect Of A Sub-Caliber Cylinder After-Body On The Behavior Of Spin-Stabilized Projectiles.	Sep 75	B008388L
BRL Memorandum Report No. 2563	Characteristics Of The Sidewall And Floor Boundary Layers In BRL Supersonic Wind Tunnel No. 1.	Dec 75	B008566L
BRL Memorandum Report No. 2573	Three-Dimensional Boundary Layer Research As Applied To The Magnus Effect On Spinning Projectiles.	Dec 75	B008821L
BRL Memorandum Report No. 2646	Muzzle-Blast Influence On Trajectory Of Asymmetrical Fin- Stabilized Projectiles.	Aug 76	B012784L
BRL Memorandum Report No. 2686	Investigations Of Transitional Ballistics In Muzzle Jet Flow Simulators.	Sep 76	B014175L
BRL Memorandum Report No. 2687	A Transient Experiment Using A Multiple-Pulse Laser Light Source.	Sep 76	B014426L
BRL Memorandum Report No. 2688	On The Free-Electron Density In A Nuclear-Blast Environment.	Sep 76	B014240L

DRDAR-TSB
SUBJECT: Change of Distribution Statement

8 March 1978

<u>REPORT</u>	<u>TITLE</u>	<u>DATE</u>	<u>AD NO</u>
BRL Technical Note No. 1541	Kinematic Evaluation Of The Special Purpose Individual Weapon Prototypes.	Aug 64	353233
BRL Technical Note No. 1691	Talk To Cadets Of The United States Military Academy, April 1968, Special Purpose Individual Weapon (SPIW).	Apr 68	390618

FOR THE DIRECTOR:



VERNON J. WYATT
Chief
Technical Support Division